

The contribution of oceanic halocarbons to marine and free troposphere air over the tropical West Pacific

S. Fuhlbrügge¹, B. Quack¹, S. Tegtmeier¹, E. Atlas², H. Hepach¹, Q. Shi³, S. Raimund¹, K. Krüger⁴

[1] GEOMAR | Helmholtz Centre for Ocean Research Kiel

[2] Rosenstiel School for Marine and Atmospheric Sciences, Miami, Florida

[3] Department of Oceanography - Dalhousie University, Halifax, Canada

[4] University of Oslo, Oslo, Norway

Correspondence to: K. Krüger (kirstin.krueger@geo.uio.no)

Response to Referee #1

Referee #1- general comment:

This paper describes a rather comprehensive set of measurements performed in the region of the South China and Sulu Seas that were designed to improve our understanding of the fluxes of three short-lived halogenated hydrocarbons from the ocean to the free troposphere. This is an important region for understanding the input of naturally emitted bromine and iodine to the stratosphere and is woefully under-sampled. Furthermore, the authors have brought many useful resources and ancillary observations to the experiment in addition to just atmospheric mixing ratio measurements to improve our understanding of halocarbon fluxes in this region. Unfortunately, I found the paper very difficult to read and follow. After hours of studying it I was still unsure that the conceptual framework of and conclusions drawn from the simple box-modelling approach were appropriate. I'm concerned with oversimplification of the processes involved. Some of this confusion stems from the language used in the paper. Descriptions often use jargon or short-cut terms that confuse rather than clarify the arguments being presented. Statements are often overly general and imprecise.

Author response to general comment:

We first would like to thank the reviewer 1 for reviewing the manuscript and for the overall positive evaluation of the paper, which she/he describes as a comprehensive addition to the understanding of VSLS fluxes from the ocean to the free troposphere. With the very helpful comments and tips we have streamlined the text substantially and thus improved its readability. Thus we also think that the conceptual framework and the conclusions drawn become much clearer. The changes for the revision include shifting of section 2.2.3 ("Convective energy"), 3.2 ("CAPE and humidity") and 5.1.1 ("R/V SONNE - R/A FALCON: identifying observations of the same air mass") to the supplement; shortening and rewriting of sections 2.4.2 ("VSLS source-loss estimate in the MABL"), 4.3 ("VSLS intercomparison: R/A FALCON and R/V SONNE"), 5.1 ("Timescales and intensity of vertical transport") and 5.2 ("Contribution of oceanic emissions to VSLS in the MABL"), 5.3.1 ("Identification of MABL air and their contained VSLS in the FT") and 5.3.3 ("Discussion"). These changes are clearly marked in the revised manuscript.

Below you find your comments (highlighted in italic) and our point-by-point answers.

Referee 1:

Confusion is enhanced by a main conclusion stated in the abstract that isn't supported by any portion of the text (line 23): "bromoform in the FT above the region originates [sic] almost entirely from the local South China Sea area", despite numbers in the summary that indicate local contributions to free troposphere CHBr₃ of 60%, which to me isn't "almost entirely" (see lines 20-26, p. 17917—is the word "originates" meant?). Perhaps some schematics or diagrams showing the magnitudes of fluxes would help. In short, there is substantial room for improving communication of the simple modelling framework so as to enhance the value of the manuscript to potential future readers.

Author response:

We agree that “almost entirely” is overstated for 60 % contribution and are now giving only the number itself (60%). We further changed “origins” to “originates”. We agree that a sketch of the fluxes and the involved budget would be very helpful. Thus we suggest replacing the former Figure 11 in the submitted manuscript with the following:

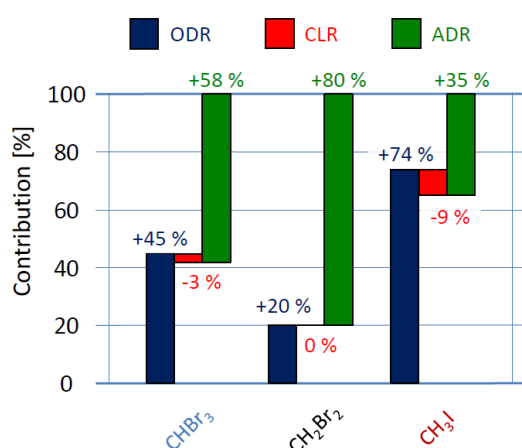


Figure 11: Budgets of the Oceanic Delivery Ratio (ODR, blue), Chemical Loss Ratio (CLR, red) and Advective Delivery Ratio (ADR, green) of CHBr₃, CH₂Br₂ and CH₃I.

Other items: Section 2.3, to what degree are conclusions based on the particular air-sea exchange parameterization the authors have chosen (at the exclusion of others)?

We have chosen the Nightingale et al. (2000) parameterization, given its a good mean representation of available air- sea flux parametrizations, which has been discussed in many papers (e.g. Lennartz et al., 2015 ACP). We agree with the reviewer that applying other air-sea flux parameterizations as e.g. discussed by Lennartz et al. (2015) leads to different fluxes (mainly for wind speeds > 10 m/s) and thus to different source-loss estimates. Thus we

compare the effect of two available air – sea flux parameterizations, one from the low (Liss and Merlivat, 1986) and one from the high end of reported parameterizations (Wanninkhof and McGillis, 1999), and included the uncertainty analysis in our discussion (see sentence below). The main conclusions of the paper do not change mainly due to overall moderate wind speed (~ 6 m/s) observed during the cruise:

“Different parameterizations for the transfer coefficient k_w such as Liss and Merlivat (1986) , which is at the lower end of reported parameterizations, and Wanninkhof and McGillis (1999), which is at the higher end, are discussed in Lennartz et al. (2015). Both lead to a reduction of the oceanic contribution to the atmospheric mixing ratios at the observed average moderate wind speeds (~6m s⁻¹) when applied to our data. Still, the general conclusion that local oceanic sources of CHBr₃ and CH₃I significantly contribute to MABL mixing ratios remains for the cruise. In times of possible higher wind speeds (>10 ms⁻¹), which are likely for this region, the flux variations between the different parameterizations but also the oceanic contribution to atmospheric abundances would increase.”

Lifetimes: are the simple lifetimes calculated for this region of the globe and season of year? Are they a mean over 24 hrs? How do clouds affect trace gas lifetimes in this region and might they explain some of the underestimations of calculated mixing ratios (particularly for CH₃I)?

In the submitted manuscript we used average tropical ($\pm 20^\circ$ latitude) lifetimes for the MABL from model runs by Hossaini et al. (2010) including degradation by photolysis and OH. According to the comment of Reviewer 2, we now use mean tropical MABL and mid tropospheric (at 10 km altitude, given in the brackets) lifetimes from Chapter 1 of the WMO (Carpenter et al., (2014)): 15 (17) days for bromoform, 94 (150) days for dibromomethane and 4 (3.5) days for methyl iodide. The manuscript is changed accordingly. All lifetimes are annually averaged, which is added to the manuscript as well.

We agree that clouds may influence the atmospheric lifetimes of the compounds via changing photolysis rates (Tie et al., 2003) as well as varying OH fields (Rex et al., 2014). Thus we added the following sentences to the discussion of the uncertainties:

“Additional uncertainties may arise from cloud induced effects on photolysis rates (Tie et al., 2003) and OH levels (Rex et al., 2014) impacting the VSLs lifetimes.”

Section 4.1 Line 5-6: mixing ratios are higher afterwards and winds speeds are lower (not higher?).

We have shortened and clarified the sentence in the following way:

“Overall, the three VSLs show a joint pattern of atmospheric mixing ratios along the cruise track with lower atmospheric surface abundances before 21 November 2011 and higher mixing ratios afterwards, which can be attributed to a change in air mass origin (Figure 1).”

Last paragraph: any discussion of age of air inferred from the ratio of two gases (CH_2Br_2 and CHBr_3) seems to require some consideration of the magnitude and variability in the emission ratio. Fortunately, you have measured emissions for both chemicals in this region to provide some information, if one presumes that ratio and variability are appropriate for a much broader region. How variable is their emission ratio and how do the ratios of measured atmospheric mixing ratios compare to this variability? A glance at figure 6d seems to indicate that there is enough variability in their emission ratio in this region of the globe that any discussion of age of air based on the ratio of the ambient mixing ratios of these gases could be not defensible.

We agree that the water concentrations and the emissions hold a large variability along the diverse cruise track. However, inspecting the variability of the ratio for given regimes along the cruise track may give insights into the “relative distance” to oceanic sources, which have often been reported to have a ratio of 0.1 between bromoform and dibromomethane directly at the source (e.g. Yokouchi et al., 2005 and references therein). As dibromomethane and bromoform have different lifetimes, the ratio decreases with a distance from the source. Thus we believe that the ratio between the two gases differentiates between air masses that were subject to the influence of fresher sources, often coastal, versus the influence of more remote air masses. We removed the “age” term and reduced the discussion to an overall description: “The concentration ratio of CH_2Br_2 and CHBr_3 (Figure 4b) has been used as an indicator for the relative distance to the oceanic source, where a ratio of 0.1 was observed crossing strong coastal source regions (Yokouchi et al., 2005; Carpenter et al., 2003). The ten times elevated CHBr_3 has a much shorter lifetime, thus degrades more rapidly than CH_2Br_2 , which increases the ratio during transport. Overall, the mean concentration ratio of CH_2Br_2 and CHBr_3 is 0.6 ± 0.2 , which suggests that predominantly older air masses are advected over the South China Sea”.

Section 4.2 I find it quite surprising and interesting that in this region of supposedly high natural emissions of VSLs the authors suggest that the highest emissions are apparently associated with anthropogenic influences and river outflow. This seems a significant point

that I haven't been aware of being made previously. Can the authors add some additional explanation and provide hard evidence from the observations made during this experiment to support this assertion? Do any previous studies support these assertions?

Elevated bromoform is found in chlorinated and ozonised waste water, from e.g. cooling plants and municipal effluents. High concentrations are also often measured at coastlines, due to either natural emissions, mainly from macro algae or due the above described anthropogenic input (see Quack and Wallace, 2003 and references therein). Therefore a plausible explanation for the elevated bromoform concentrations, measured within the contaminated Singapore Strait is a likely influence by anthropogenic effluents. Elevated bromoform concentrations close to Bornean coastal sites and cities with river run-off and its negative correlation with salinity indicate riverine sources for the compound. While it is therefore clear that riverine transport from coastal or inland sites is the cause for the elevated coastal concentrations, it cannot be completely resolved, whether anthropogenic sources alone are responsible or whether coastal natural sources may contribute as well. We clarified the text in this regard and changed it to:

“Along the west coast (November 19 - 23, 2011) and northeast coast of Borneo (November 25, 2011), bromocarbon concentrations are elevated, and especially CHBr₃ concentrations increase in waters with lower salinities, indicating an influence by river run off. Elevated CHBr₃ concentrations are often found close to coasts with riverine inputs caused by natural sources and industrial and municipal effluents (e.g. Quack and Wallace, 2003; Fuhlbrügge et al., 2013 and references therein).”

Section 4.3: an indication of the number of comparison measurements and an uncertainty on the values being compared (in the text and in Table 2) is lacking but would be useful. Line 20-24. Regarding the intercomparison, I would think any interpretation of gradients between the free troposphere and the boundary layer should be done with data that are internally consistent so that any potential instrumental influences don't affect the conclusions. In that respect, I don't understand why the mean of the different measurement techniques onboard the aircraft (and that have substantial differences that would seem to be instrumental) is used to compare with the ship-board marine bl results. In a discussion of mean results, sure, mention results from both instruments. But when gradients are being interpreted, it seems only appropriate to use aircraft results that are consistent with those from the ship (good to see that the unbiased result appears in figure 13).

We agree with the reviewer and included the information in the manuscript. We added the corresponding numbers in Table 1 and 2 (Falcon GhOST: n=513, WASP: n=202; SONNE: N=195).

According to Sala et al. (2014) the agreement between the GhOST and WASP instruments for the bromocarbons are within the expected uncertainty range of both instruments. Next to this, WASP measurements were available only up to 6 km altitude and for the bromocarbons. Thus, using measurements from both instruments benefits a larger spatial and temporal resolution of the data set which is considered representative for the region. A possible instrumental offset for CH₃I is discussed. We rewrote lines 16-24 on page 17922 to:

“According to Sala et al. (2014) the agreement between the GhOST and WASP instruments are within the expected uncertainty range of both instruments which is then assumed to be also valid for the ship measurements. The good agreement between WASP and ship data might be caused by the same sampling and analysis method, both using stainless steel canisters and subsequent analysis with GC/MS, while GhOST measures in-situ in a different resolution. Since GhOST and WASP measurements together cover a larger spatial area and higher temporal resolution, a mean of both measurements is used in the following for computations in the free troposphere. For CH₃I significantly higher mixing ratios were measured during the meetings between ship and aircraft (Table 2). Whether this offset is systematic for the different methods, needs further investigation.

Figures: 6d, I'd like to be able to see the CH₂Br₂ results, but they are often obscured by other data.

We improved the visibility of CH₂Br₂ lines in the former Figure 6 (now Figure 4) by choosing a darker line for them and using non-linear y-axes.

Figure 8, consider making the legend more informative by indicating ship, flask, insitu instead of the instrument acronyms.

According to your suggestions we added the information to the figure legend of the former Figure 8, now Figure 6.

Figure 13, I presume the unadjusted observations from the aircraft are the mean of the two available measurements and the adjust ones are only the data from aircraft flasks? Explicitly stating so would help.

Yes, thanks for pointing this out. We further explain details in the figure caption now. Unadjusted measurements include measurements from both instruments on the aircraft. The “adjustment” only accounts for methyl iodide. Since flask (WASP) observations are not available for methyl iodide, the in-situ observations are reduced by the percentage of which in-situ measurements on the aircraft and on the ship differed during the two meetings on November 19 and 21, 2011, according to Table 2:

“Mean FT mixing ratios (solid lines) and 1 standard deviation (shaded areas) from in-situ and flask observations on R/A FALCON (Obsv., black) versus simulated mean FT mixing ratios from MABL air (MABL, red) and oceanic emissions (Ocean, blue) observed by R/V SONNE. R/A FALCON in-situ observations have been adjusted for CH₃I (Obsv.*, dashed black) according measurements deviations during the meetings of R/V SONNE and R/A FALCON (compare Table 2; Section 4.3).”

References

Carpenter, L., Liss, P., and Penkett, S.: Marine organohalogens in the atmosphere over the Atlantic and Southern Oceans, *Journal of Geophysical Research-Atmospheres*, 108, 10.1029/2002JD002769, 2003.

Carpenter, L. J., Reimann, S., Burkholder, J. B., Clerbaux, C., Hall, B. D., Hossaini, R., Laube, J. C., and Yvon-Lewis, S. A.: Update on Ozone-Depleting Substances (ODSs) and Other Gases of Interest to the Montreal Protocol, in: *Scientific Assessment of Ozone Depletion: 2014*, edited by: Engel, A., and Montzka, S. A., World Meteorological Organization, Geneva, 2014.

Fuhlbrügge, S., Krüger, K., Quack, B., Atlas, E., Hepach, H., and Ziska, F.: Impact of the marine atmospheric boundary layer conditions on VSLS abundances in the eastern tropical and subtropical North Atlantic Ocean, *Atmospheric Chemistry and Physics*, 13, 6345-6357, 10.5194/acp-13-6345-2013, 2013.

Hossaini, R., Chipperfield, M., Monge-Sanz, B., Richards, N., Atlas, E., and Blake, D.: Bromoform and dibromomethane in the tropics: a 3-D model study of chemistry and transport, *Atmospheric Chemistry and Physics*, 10, 719-735, 10.5194/acp-10-719-2010, 2010.

Lennartz, S. T., Krysztofiak, G., Marandino, C. A., Sinnhuber, B. M., Tegtmeier, S., Ziska, F., Hossaini, R., Krüger, K., Montzka, S. A., Atlas, E., Oram, D. E., Keber, T., Bönisch, H.,

and Quack, B.: Modelling marine emissions and atmospheric distributions of halocarbons and dimethyl sulfide: the influence of prescribed water concentration vs. prescribed emissions, *Atmos. Chem. Phys.*, 15, 11753-11772, 10.5194/acp-15-11753-2015, 2015.

Liss, P. S., and Merlivat, L.: Air-Sea Gas Exchange Rates: Introduction and Synthesis, in: *The Role of Air-Sea Exchange in Geochemical Cycling*, edited by: Buat-Menard, P., Reidel, D., and Norwell, M., Springer Netherlands, 113-127, 1986.

Nightingale, P., Malin, G., Law, C., Watson, A., Liss, P., Liddicoat, M., Boutin, J., and Upstill-Goddard, R.: In situ evaluation of air-sea gas exchange parameterizations using novel conservative and volatile tracers, *Global Biogeochemical Cycles*, 14, 373-387, 10.1029/1999GB900091, 2000.

Quack, B., and Wallace, D.: Air-sea flux of bromoform: Controls, rates, and implications, *Global Biogeochemical Cycles*, 17, 10.1029/2002GB001890, 2003.

Rex, M., Wohltmann, I., Ridder, T., Lehmann, R., Rosenlof, K., Wennberg, P., Weisenstein, D., Notholt, J., Kruger, K., Mohr, V., and Tegtmeier, S.: A tropical West Pacific OH minimum and implications for stratospheric composition, *Atmospheric Chemistry and Physics*, 14, 4827-4841, 10.5194/acp-14-4827-2014, 2014.

Sala, S., Bonisch, H., Keber, T., Oram, D., Mills, G., and Engel, A.: Deriving an atmospheric budget of total organic bromine using airborne in situ measurements from the western Pacific area during SHIVA, *Atmospheric Chemistry and Physics*, 14, 6903-6923, 10.5194/acp-14-6903-2014, 2014.

Tie, X., Madronich, S., Walters, S., Zhang, R., Rasch, P., and Collins, W.: Effect of clouds on photolysis and oxidants in the troposphere, *Journal of Geophysical Research-Atmospheres*, 108, 10.1029/2003JD003659, 2003.

Wanninkhof, R., and McGillis, W.: A cubic relationship between air-sea CO₂ exchange and wind speed, *Geophysical Research Letters*, 26, 1889-1892, 10.1029/1999GL900363, 1999.

Yokouchi, Y., Hasebe, F., Fujiwara, M., Takashima, H., Shiotani, M., Nishi, N., Kanaya, Y., Hashimoto, S., Fraser, P., Toom-Saunty, D., Mukai, H., and Nojiri, Y.: Correlations and emission ratios among bromoform, dibromochloromethane, and dibromomethane in the atmosphere, *Journal of Geophysical Research-Atmospheres*, 110, 10.1029/2005JD006303, 2005.

Response to Referee #2

We would like to thank reviewer 2 for reviewing the manuscript. Below you find our point-by-point answers to your comments (highlighted in italic).

Referee #2:

The contribution of oceanic halocarbons to marine and free troposphere air over the tropical West Pacific by Fuhlbrügge et al. This paper presents seawater and atmospheric measurements of CHBr₃, CH₂Br₂ and CH₃I obtained during the ship cruise and aircraft campaign of the SHIVA project. Samples were obtained around Borneo in November-December 2011 and are used here to derive ocean emission fluxes in the region and, with the aid of transport modelling, the contribution of the above gases to the free troposphere. Given the likely importance of this region for the transport of air masses to the stratosphere, and given that the region is poorly sampled (in terms of VSLS), this paper is a useful addition to the literature, providing a good synthesis of the SHIVA measurements. I have no major objections to the method and therefore recommend the paper for publication.

My main concern with the paper is that I found it extremely difficult to read and somewhat convoluted in many parts. I encourage the authors to carefully check the manuscript for places where the text could be streamlined to improve readability and where the main messages could be distilled to avoid them being diluted by so many numbers and detail. I had to stop listing technical corrections given the sheer enormity of the task.

We first thank the reviewer for the general positive evaluation of the paper, which she/he describes as a useful addition to the literature. We agree with the reviewer that the text can be written more concisely and distilled to improve readability, if we omit explaining all details of the method which may have convoluted the main messages. Thus, we intensively revised the paper to streamline it and to make it easier to read and follow. The changes for the revision include shifting of section 2.2.3 (“Convective energy”), 3.2 (“CAPE and humidity”) and 5.1.1 (“R/V SONNE - R/A FALCON: identifying observations of the same air mass”) to the supplement; shortening and substantial rewriting of sections 2.4.2 (“VSLS source-loss estimate in the MABL”), 4.3 (“VSLS intercomparison: R/A FALCON and R/V SONNE”), 5.1 (“Timescales and intensity of vertical transport”) and 5.2 (“Contribution of oceanic emissions to VSLS in the MABL”), 5.3.1 (“Identification of MABL air and their contained

VSLs in the FT”) and 5.3.3 (“Discussion”). These changes are clearly marked in the revised manuscript. We also have asked a native speaker for revisions of the language.

I also encourage the authors to check that the most appropriate citations are given throughout the manuscript. Citing older classic papers is fine (and good) but in many places the discussion would be better served by citing the most up-to-date literature in addition. For example, in the introduction numbers are given for the “mean atmospheric lifetime” of CHBr₃, CH₂Br₂ and CH₃I. I don’t understand why the authors refer to such old papers here (Ko et al. 2003 and Solomon et al. 1994) when the most recent and comprehensive evaluation of the lifetimes of these compounds is given in the 2014 WMO O₃ Assessment (Chapter 1: Carpenter and Reimann et al.). The concept of a mean atmospheric lifetime for VSLs can be somewhat problematic. I suggest quoting the tropical MBL local lifetime and range from the 2014 report.

We replaced the mean MABL and mid tropospheric lifetimes to mean tropical MABL and mid tropospheric (at 10 km altitude, given in the brackets) lifetimes and also added the reported lifetime range from Chapter 1 of the WMO (Carpenter et al., (2014)):

“Annually averaged mean tropical lifetimes of these halogenated very short-lived substances (VSLs) in the boundary layer are 15 (range: 13 – 17) days for CHBr₃, 94 (84 – 114) days for CH₂Br₂ and 4 (3.8 – 4.3) days for CH₃I. The according mean tropospheric lifetimes at 10 km height are 17 (16 – 18) days, 150 (144 – 155) days, respectively 3.5 (3.4 – 3.6) days (Carpenter et al., 2014).”

Due to these new lifetimes the former Figure 12, (now 10) and Figure 13 (now 11) and the Table 3, 4, 5 and A1 (now S-Table 1) have been changed and the corresponding text was adjusted to it (Sections 5.2 and 5.3).

Abstract:

Line 10: The sentence beginning “Elevated oceanic concentrations..” is long. Consider using the word “respectively” in the second half; i.e. change to “... with high corresponding oceanic emissions of 1486, 405, and 433, respectively, characterize..”

We agree and shortened the sentence to: “Elevated oceanic concentrations for bromoform, dibromomethane and methyl iodide of on average 19.9, 5.0 and 3.8 pmol L⁻¹ in particular close to Singapore and at the coast of Borneo with high corresponding oceanic emissions of 1486, 405 and 433 pmol m⁻² h⁻¹, respectively, characterize this tropical region as a strong source of these compounds. Atmospheric mixing ratios in the MABL were unexpectedly

relatively low with 2.08, 1.17 and 0.39 ppt for bromoform, dibromomethane and methyl iodide.”

Line 24: Change “origins” to “originates”

Done.

Introduction:

Line 2: Change “the atmospheric ozone” to “atmospheric ozone” Add “e.g.” before citations to Solomon (1999) and Saiz-Lopez and von Glasow (2012).

Done.

Line 4: Change “via photochemical and heterogeneous reaction cycles from” to “following the photochemical breakdown of”.

Thanks, done.

Line 14: Change “the halogenated very short lived substances” to “these halogenated very short-lived substances”.

Done.

Line 16: “Climate change could strongly affect marine biota. . . “. Are there not other recent papers that also suggest this? For example: Hughes, C., et al. (2012), ‘Climate induced change in biogenic bromine emissions from the Antarctic marine biosphere’, Global Biogeochem. Cycles.

We added Hughes et al. (2012), Leedham et al. (2013) and Hepach et al. (2014), who reported on possible influences of climate change on marine halocarbon production leading to enhanced oceanic production and oceanic emissions of brominated and iodinated compounds: “Climate change could strongly affect marine biota and thereby halogen sources and the oceanic emission strength (Hughes et al., 2012; Leedham et al., 2013; Hepach et al., 2014).”

Line 23: Change “methyl iodide” to “CH₃I”. Generally, why bother keep using the full names bromoform, dibromomethane and methyl iodide throughout the text once they have been defined? Check full text and at least be consistent.

The idea of using the full names throughout the manuscript was to make it easier to understand for non-chemists, since chemical formulas generally tend to confuse these

readers. Nevertheless, we searched through the whole manuscript and kept on using the chemical formulas consistently now.

Line 25: The sentence beginning “Significantly lower. . .” should be amended. Why talk about just model runs looking at the impact of bromine when the previous discussion was iodine-focused. Numerous recent papers from the Saiz-Lopez group have examined the impact of bromine and iodine on tropospheric O₃ (e.g. Saiz-Lopez et al. 2014, iodine chemistry in the troposphere and its effect on ozone, ACP, 2014). As we are talking about VSLs in this paper, an appropriate citation would also be to Hossaini et al. (2015, Nature Geoscience) who examined their impact on UTLS O₃. Please include these additional citations and add “e.g.” before the list.

We included the suggested references and changed the text to:

“Recent studies reported significant contributions of bromine and iodine to the total rate of tropospheric and stratospheric ozone loss (e.g. von Glasow et al., 2004; Yang et al., 2005; Saiz-Lopez et al., 2014; Yang et al., 2014; Hossaini et al., 2015).”

Line 17: The sentence beginning “The goal of SHIVA” is odd. Was that really the main objective? Consider “was to combine observations of VSLs and models to better understand the processes contributing to ozone loss in the stratosphere and how such factors could respond to climate change.” This seems more accurate to me.

Thanks, this part has now been removed for further streamlining of the manuscript.

Data and Methods:

Why does the sub-sub section “2.1.2 Aircraft campaigns” come under the SHIVA SONNE subsection? Could Section 2.1 simply be named something like “Overview of ship cruise and aircraft campaign”? Given the length of these sections, I don’t think the subsections are needed.

We agree and renamed section 2.1 to “Ship cruise and aircraft campaign”. Section 2.1.1 and 2.1.2 were merged into section 2.1.

Section 4.2:

Line 20: Is it possible to comment more on the possible different sources for CH₃I compared to the bromocarbons here?

Methyl iodide has different sources, e.g. phytoplankton, macro algae and photochemical production, the latter is assumed to drive the major part of the sea – air flux of CH₃I (e.g. Manley and Dastoor, 1988; Manley and de la Cuesta, 1997; Richter and Wallace, 2004). This is added to Section 4.2 now. We try to summarize different possible sources, however the statements remain speculative. Still the fact, that methyl iodide reveals a different pattern than the other two compounds indicate different source and/or loss processes. We clarified this in the manuscript:

“CH₃I concentrations range from 0.6 – 18.8 pmol L⁻¹ with a mean of 3.8 pmol L⁻¹ and show a different distribution along the ship track which might be ascribed to additional photochemical production of CH₃I in the surface waters (e.g. Manley and Dastoor, 1988; Manley and de la Cuesta, 1997; Richter and Wallace, 2004).”

Line 27 on river run: This point needs expanding. Why would the bromocarbons be elevated due to river run and how is the influence of river run detected?

See also our response to anonymous Reviewer 1: Elevated bromoform is found in chlorinated and ozonised waste water, from e.g. cooling plants and municipal effluents. High concentrations are also often measured at coastlines, due to either natural emissions, mainly from macro algae or due the above described anthropogenic input (see Quack and Wallace, 2003 and references therein). Therefore a plausible explanation for the elevated bromoform concentrations, measured within the contaminated Singapore Strait is a likely influence by anthropogenic effluents. Elevated bromoform concentrations close to Bornean coastal sites and cities with river run-off, and its negative correlation with salinity, indicate riverine sources for the compound. While it is therefore clear that riverine transport from coastal or inland sites is the cause for the elevated coastal concentrations, it cannot be completely resolved, whether anthropogenic sources alone are responsible or whether coastal natural sources may contribute as well. We clarified the text in this regard and changed it to:

“Along the west coast (November 19 - 23, 2011) and northeast coast of Borneo (November 25, 2011), bromocarbon concentrations are elevated, and especially CHBr₃ concentrations increase in waters with lower salinities, indicating an influence by river run off. Elevated CHBr₃ concentrations are often found close to coasts with riverine inputs caused by natural sources and industrial and municipal effluents (e.g. Quack and Wallace, 2003; Fuhlbrügge et al., 2013 and references therein).”

Discussion:

Line 10: WMO (2015) should be WMO (2014)

We changed the reference to Carpenter et al. (2014).

References

Carpenter, L. J., Reimann, S., Burkholder, J. B., Clerbaux, C., Hall, B. D., Hossaini, R., Laube, J. C., and Yvon-Lewis, S. A.: Update on Ozone-Depleting Substances (ODSs) and Other Gases of Interest to the Montreal Protocol, in: Scientific Assessment of Ozone Depletion: 2014, edited by: Engel, A., and Montzka, S. A., World Meteorological Organization, Geneva, 2014.

Fuhlbrügge, S., Krüger, K., Quack, B., Atlas, E., Hepach, H., and Ziska, F.: Impact of the marine atmospheric boundary layer conditions on VSLS abundances in the eastern tropical and subtropical North Atlantic Ocean, *Atmospheric Chemistry and Physics*, 13, 6345-6357, 10.5194/acp-13-6345-2013, 2013.

Hepach, H., Quack, B., Ziska, F., Fuhlbrügge, S., Atlas, E., Krüger, K., Peeken, I., and Wallace, D. W. R.: Drivers of diel and regional variations of halocarbon emissions from the tropical North East Atlantic, *Atmos. Chem. Phys.*, 14, 10.5194/acp-14-1255-2014, 2014.

Hossaini, R., Chipperfield, M., Montzka, S., Rap, A., Dhomse, S., and Feng, W.: Efficiency of short-lived halogens at influencing climate through depletion of stratospheric ozone, *Nature Geoscience*, 8, 186-190, 10.1038/NGEO2363, 2015.

Hughes, C., Johnson, M., von Glasow, R., Chance, R., Atkinson, H., Souster, T., Lee, G., Clarke, A., Meredith, M., Venables, H., Turner, S., Malin, G., and Liss, P.: Climate-induced change in biogenic bromine emissions from the Antarctic marine biosphere, *Global Biogeochemical Cycles*, 26, 10.1029/2012GB004295, 2012.

Leedham, E., Hughes, C., Keng, F., Phang, S., Malin, G., and Sturges, W.: Emission of atmospherically significant halocarbons by naturally occurring and farmed tropical macroalgae, *Biogeosciences*, 10, 3615-3633, 10.5194/bg-10-3615-2013, 2013.

Manley, S., and Dastoor, M.: Methyl-iodide (CH₃I) production by kelp and associated microbes, *Marine Biology*, 98, 477-482, 10.1007/BF00391538, 1988.

Manley, S. L., and de la Cuesta, J. L.: Methyl iodide production from marine phytoplankton cultures, *Limnology and Oceanography*, 42, 142-147, 1997.

465 Quack, B., and Wallace, D.: Air-sea flux of bromoform: Controls, rates, and implications,
 466 Global Biogeochemical Cycles, 17, 10.1029/2002GB001890, 2003.

467 Richter, U., and Wallace, D.: Production of methyl iodide in the tropical Atlantic Ocean,
 468 Geophysical Research Letters, 31, 10.1029/2004GL020779, 2004.

469 Saiz-Lopez, A., Fernandez, R., Ordonez, C., Kinnison, D., Martin, J., Lamarque, J., and
 470 Tilmes, S.: Iodine chemistry in the troposphere and its effect on ozone, Atmospheric
 471 Chemistry and Physics, 14, 13119-13143, 10.5194/acp-14-13119-2014, 2014.

472 von Glasow, R., von Kuhlmann, R., Lawrence, M., Platt, U., and Crutzen, P.: Impact of
 473 reactive bromine chemistry in the troposphere, Atmospheric Chemistry and Physics, 4, 2481-
 474 2497, 2004.

475 Yang, X., Cox, R., Warwick, N., Pyle, J., Carver, G., O'Connor, F., and Savage, N.:
 476 Tropospheric bromine chemistry and its impacts on ozone: A model study, Journal of
 477 Geophysical Research-Atmospheres, 110, 10.1029/2005JD006244, 2005.

478 Yang, X., Abraham, N., Archibald, A., Braesicke, P., Keeble, J., Telford, P., Warwick, N.,
 479 and Pyle, J.: How sensitive is the recovery of stratospheric ozone to changes in
 480 concentrations of very short-lived bromocarbons?, Atmospheric Chemistry and Physics, 14,
 481 10431-10438, 10.5194/acp-14-10431-2014, 2014.

Relevant changes made in the manuscript:

- Substantially streamlined
- Shifted section 2.2.3 (“Convective energy”), 3.2 (“CAPE and humidity”) and 5.1.1 (“R/V SONNE - R/A FALCON: identifying observations of the same air mass”) to the supplement
- Shortening and rewriting of sections 2.4.2 (“VSLs source-loss estimate in the MABL”), 4.3 (“VSLs intercomparison: R/A FALCON and R/V SONNE”), 5.1 (“Timescales and intensity of vertical transport”) and 5.2 (“Contribution of oceanic emissions to VSLs in the MABL”), 5.3.1 (“Identification of MABL air and their contained VSLs in the FT”) and 5.3.3 (“Discussion”)
- Updating our results with most current lifetime estimates of bromoform, dibromomethane and methyl iodide from the WMO, 2014.
- Figures:
 - Figure 1b is now Figure 2a
 - Figure 3 is now S-Figure 1
 - Figure 4 is now Figure 3a
 - Figure 5 is now Figure 3b, in addition we revised the colours and colour-bar
 - Figure 6 is now Figure 4, in addition we overworked the Figure by using non-linear y-axis
 - Figure 7 is now Figure 5
 - Figure 8 is now Figure 6, in addition we added “in-situ” and “flask” to the legend
 - Figure 9 is now Figure 7, in addition the colour-scale was extended to 10 days
 - Figure 10 is now Figure 8
 - Figure 11 is now Figure 9, in addition the former ODR time series has been replaced by an ODR budget sketch.
 - Figure 12 is now Figure 10
 - Figure 13 is now Figure 11

All changes are marked-up (removed: red, rewritten: blue, shifted: green) in the following:

Abstract

Emissions of halogenated very short lived substances (VSLS) from the ~~tropical~~ oceans contribute to the atmospheric halogen budget and affect tropospheric and stratospheric ozone. Here we investigate the contribution of natural oceanic VSLS emissions to the Marine Atmospheric Boundary Layer (MABL) and their transport into the Free Troposphere (FT) over the tropical West Pacific. The study concentrates ~~in particular on ship and aircraft measurements of the VSLS~~ bromoform, dibromomethane and methyl iodide ~~and meteorological parameters measured on ship and air craft~~ during the SHIVA (Stratospheric Ozone: Halogen Impacts in a Varying Atmosphere) campaign in the South China and Sulu Seas in November 2011. Elevated oceanic concentrations for bromoform, dibromomethane and methyl iodide of on average 19.9, 5.0 and 3.8 pmol L⁻¹ in particular close to Singapore and at the coast of Borneo with high corresponding oceanic emissions of 1486, 405 and 433 pmol m⁻² h⁻¹, respectively, characterize this tropical region as a strong source of these compounds. Atmospheric mixing ratios in the MABL were unexpectedly relatively low with 2.08, 1.17 and 0.39 ppt for bromoform, dibromomethane and methyl iodide. We use meteorological and chemical ship and aircraft observations, FLEXPART trajectory calculations and source-loss estimates to identify the oceanic VSLS contribution to the MABL and to the FT. Our results show that ~~a convective,~~ the well-ventilated MABL and intense convection led to the low atmospheric mixing ratios in the MABL despite the high oceanic emissions. ~~in coastal areas of the South China and Sulu Seas. While t~~ Most of the accumulated bromoform in the FT above the region originates ~~almost entirely mainly~~ from the local South China Sea area (up to 60 %), while dibromomethane is largely advected from distant source regions. The accumulated ~~FT mixing ratio of~~ methyl iodide in the FT is higher than can be explained with ~~the local oceanic or MABL~~ contributions. Possible reasons, uncertainties and consequences of our observations and model estimates are discussed.

1. Introduction

Halogens play an important role for atmospheric chemical processes. ~~The contribution of halogens to the atmospheric ozone chemistry is well known. Besides Halogen-Chlorine,~~ bromine and iodine radicals destroy ozone in the stratosphere (e.g. Solomon, 1999) and also affect tropospheric chemistry (e.g. Saiz-Lopez and von Glasow, 2012). Halogens are released following the photochemical breakdown of ~~via photochemical and heterogeneous reaction cycles from~~ organic ~~halogenated~~ anthropogenic and natural trace gases. ~~, originating from anthropogenic and natural sources, including macro algae, seaweed, phytoplankton and other~~

~~marine biota.~~ A large number of very short lived brominated and iodinated organic substances, originating from macro algae, seaweed, phytoplankton and other marine biota, are emitted from tropical oceans and coastal regions to the atmosphere (Gschwend et al., 1985; Carpenter and Liss, 2000; Quack and Wallace, 2003; Quack et al., 2007; Liu et al., 2013). In particular, marine emissions of bromoform (CHBr_3), dibromomethane (CH_2Br_2) and methyl iodide (CH_3I) are major contributors of ~~organic~~ bromine and iodine to the atmosphere (Montzka and Reimann, 2011). Annually averaged mean ~~tropical atmospheric~~ lifetimes of these halogenated very short-lived substances ~~the halogenated very short-lived substances~~ (VSLs) in the boundary layer ~~and in the~~ are 26–15 (range: 13 – 17) days for CHBr_3 ~~bromoform~~, 120–94 (84 – 114) days for CH_2Br_2 ~~dibromomethane~~ (Ko et al., 2003) and 4 (3.8 – 4.3) days for CH_3I ~~methyl iodide~~ (Carpenter et al., 2014) (Solomon et al., 1994). The mean tropospheric lifetimes of these compounds at 10 km height are 17 (16 – 18) days, 150 (144 – 155) days, respectively 3.5 (3.4 – 3.6) days (Carpenter et al., 2014). Climate change could strongly affect marine biota and thereby halogen sources and the oceanic emission strength (Hughes et al., 2012; Leedham et al., 2013; Hepach et al., 2014).

Aircraft measurements from Dix et al. (2013) suggest that the halogen-driven ozone loss in the Free Troposphere (FT) is currently underestimated. In particular, ~~significant~~ elevated amounts of the iodine oxide free radical (IO) ~~were found~~ in the FT over the Central Pacific ~~suggesting~~ that iodine ~~has a much~~ may have a larger effect on the FT ozone budget than currently estimated by chemical models. Coinciding with this study, Tegtmeier et al. (2013) projected a higher CH_3I ~~methyl iodide~~ delivery to the Upper Troposphere / Lower Stratosphere (UTLS) over the tropical West Pacific than previously reported, using an observation based emission climatology by Ziska et al. (2013). Recent studies reported significant contributions of bromine and iodine to the total rate of tropospheric and stratospheric ozone loss (e.g. von Glasow et al., 2004; Yang et al., 2005; Saiz-Lopez et al., 2014; Yang et al., 2014; Hossaini et al., 2015). ~~Significantly lower amounts of tropospheric and stratospheric ozone are found calculated in chemistry transport and chemistry climate model runs when taking atmospheric bromine is taken into account (von Glasow et al., 2004; Yang et al., 2005; Yang et al., 2014).~~ Deep tropical convective events (Aschmann et al., 2011; Tegtmeier et al., 2013; Carpenter et al., 2014) as well as tropical cyclones, i.e. typhoons (Tegtmeier et al., 2012), are projected to transport ~~the~~ VSLs rapidly from the ocean surface to the upper tropical tropopause layer. ~~Even though the influence of halogens on the tropospheric and stratospheric ozone chemistry is crucial~~ Despite the importance of halogens on tropospheric and stratospheric ozone chemistry, halogen sources and transport ways are

still not fully understood. While the tropical West Pacific ~~is an~~ comprises a intense strong VSL source regions ~~for VSL~~ (Krüger and Quack, 2013), only low mean atmospheric mixing ratios were observed ~~for VSL in the Eastern and Southeast China Seas~~ during ship ~~cruises~~ campaigns in 1994 and 2009 (Yokouchi et al., 1997; Quack and Suess, 1999) and ~~through the tropical West Pacific~~ in 2010 (Quack et al., 2011; Brinckmann et al., 2012). None of these previous studies investigated the contribution of oceanic VSL emissions to the marine atmospheric boundary layer (MABL) and to the FT in this hot spot region with large oceanic sources and strong convective activity.

The SHIVA (‘Stratospheric Ozone: Halogen Impacts in a Varying Atmosphere’) ship, aircraft and ground-based campaign during November and December 2011 in the Southern South China and Sulu Seas investigated oceanic emission strengths of marine VSL, as well as their atmospheric transport and chemical transformation from the ocean surface to the upper troposphere. ~~The goal of SHIVA was to improve the prediction of rate, timing and sensitivity of the ozone layer recovery due to climate forcing by combining observations and models.~~ For more details about the SHIVA campaign see the ACP special issue (http://www.atmos-chem-phys.net/special_issue306.html).

In this study, we present campaign data from the research vessel (R/V) SONNE and the research aircraft (R/A) FALCON. We identify the contribution of oceanic emissions to the MABL and their exchange into the FT applying in-situ observations, trajectory calculations and source-loss estimates. The results are crucial for a better process understanding and for chemical transport model validation (Hossaini et al., 2013; Aschmann and Sinnhuber, 2013). An overview of the data and the methods used in this study is given in Chapter 2. Chapter 3 provides results from the meteorological observations along the cruise. Chapter 4 compares atmospheric VSL measurements derived on R/V SONNE and R/A FALCON ~~by different gas chromatographic / mass spectrometric (GC/MS) instruments.~~. The contribution of the oceanic emissions to the MABL and FT air is investigated and discussed in Chapter 5 ~~by applying model calculations and the field observations~~. Finally, a summary of the results is given in Chapter 6.

2. Data and Methods

2.1. ~~SHIVA SONNE~~ Overview of Ship and aircraft campaigns

~~2.1.1. Ship cruise~~

The R/V SONNE cruise ~~of R/V SONNE~~ started on November 15, 2011 in Singapore and ended on November 29, 2011 in Manila, Philippines (Figure 1 ~~Figure 1a~~). The ship crossed

the southwestern South China Sea towards the northwestern coast of Borneo from November 16 – 19, 2011. From November 19 - 23, 2011 the ship headed northeast along the northern coast of Borneo towards the Sulu Sea. Two diurnal stations took place on November 18, 2011 at 2.4° N / 110.6° E and on November 22, 2011 at 6.0° N / 114.8° E. Two meetings between ~~R/V SONNE and R/A FALCON~~ ship and aircraft were carried out on November 19 and 21, 2011, where R/A FALCON passed R/V SONNE within a distance of about 100 m ~~for~~ several times to ~~get~~ simultaneously measurements of the same air masses. On November 24, 2011 the ship entered the Sulu Sea, and after 4 days transect, R/V SONNE reached the Philippine coast.

~~2.1.2. Aircraft campaign~~

16 measurement flights were carried out with R/A FALCON between November 16 and December 11, 2011 as part of the SHIVA campaign to investigate halogenated VSLS from the surface up to 13 km altitude over the South China and Sulu Seas. Observations were performed between 1° N and 8° N, as well as 100° E and 122° E, ~~using from~~ Miri, Borneo (Malaysia) as the aircraft base. A detailed description of the VSLS measurements and flight tracks can be found in Sala et al. (2014).

2.2. Meteorological observations during SHIVA

2.2.1. Measurements on board R/V SONNE

Meteorological parameters (temperature, air pressure, humidity and wind) were recorded at 20 m height every second ~~on R/V SONNE~~. A 10 minute running mean of this data is used for ~~our investigations~~ this study. An optical disdrometer ('ODM-470') measured the amount and intensity of precipitation during the cruise at 15 m height every minute (see Supplementary Material for further details). To obtain atmospheric profiles of air temperature, relative humidity and wind from the surface to the stratosphere 67 GRAW DFM-09 and 6 GRAW DFM-97 radiosondes were launched every 6 hours at standard UTC times (0, 6, 12, 18) from the working deck of R/V SONNE at about 2 m above sea level. At the 24 h stations, the launch frequency was increased to 2 – 3 hours to analyse short term diel variations of the atmospheric boundary layer. ~~During the cruise the~~ The radiosonde data was integrated in near real time into the Global Telecommunication System (GTS) to improve meteorological reanalyses such as ERA-Interim (Dee et al., 2011), which is used as input data for the trajectory calculations (Section 5).

2.2.2. Marine atmospheric boundary layer

The MABL is the atmospheric surface layer above the ocean in which trace gas emissions are mixed vertically by convection and turbulence on a short time scale of about an hour (Stull, 1988; Seibert et al., 2000). The upper boundary of the MABL is either indicated by a stable layer e.g. a temperature inversion or by a significant reduction in air moisture. Determination of the MABL height can be achieved by theoretical approaches, e.g. using critical Bulk Richardson number (Troen and Mahrt, 1986; Vogelezang and Holtslag, 1996; Sorensen, 1998) or by practical approaches summarized in Seibert et al. (2000). An increase with height of the virtual potential temperature, the temperature an air parcel would acquire if adiabatically brought to standard surface pressure with regard to the humidity of the air parcel, identifies the base of the stable layer, which is typically found between 100 m and 3 km altitude (Stull, 1988). In this study, we use the height of the base of the stable layer increased by half of the stable layer depth as the definition for the MABL height. The height of the MABL is determined from the atmospheric profiles measured by radiosondes launched on board the ship, as described in detail by Fuhlbrügge et al. (2013).

~~2.2.3.1.1.1. Convective energy~~

~~Intense solar insolation and high sea surface temperatures (SST) favour the South China and Sulu Seas for high convective activity. To indicate atmospheric instabilities that can lead to convective events the convective available potential energy (CAPE) (Margules, 1905; Moncrieff and Miller, 1976) is calculated. CAPE is defined as the cumulative buoyant energy of an air parcel from the level of free convection (LFC), the level where the environmental temperature decreases faster than the moist adiabatic lapse rate of a saturated air parcel at the same level, and the equilibrium level (EL), the height at which the air parcel has the same temperature as the environment. CAPE is computed after Eq. 1, with g as the gravitational constant, $T_{v,p}$ as the virtual temperature of an adiabatic ascending air parcel at geometric height z , $T_{v,e}$ as the virtual temperature of the environment at z , z_{LFC} as the height of the level of free convection and z_{EL} as the height of the equilibrium level. CAPE can range from 0 to more than 3 kJ/kg for very intense thunderstorms (Thompson and Edwards, 2000).~~

$$CAPE = \int_{z_{LFC}}^{z_{EL}} g \cdot \left(\frac{T_{v,p} - T_{v,e}}{T_{v,e}} \right) dz \quad (\text{Eq. 1})$$

2.3. VSLS measurements and flux calculation

~~For the investigation of~~ VSLS abundances~~;~~ in marine surface air and sea water were sampled synchronously on R/V SONNE along the cruise track. From these data measurements ~~the~~ oceanic emissions of the compounds during the SHIVA campaign were calculated (Section 2.3.3~~2.3.3~~). Additionally, VSLS abundances ~~were~~ measured in the MABL and the FT ~~were measured~~ by R/A FALCON (Sala et al., 2014; Tegtmeier et al., 2013).

2.3.1. Atmospheric samples

Air samples were taken ~~on a~~ 3 hourly ~~basis~~ along the cruise track, and ~~in a~~ 1 – 2 hourly ~~rhythm~~ during the 24 hour stations on R/V SONNE resulting in a total of 195 samples during the cruise. The air was pressurized to 2 atm in pre-cleaned stainless steel canisters ~~using~~ with a metal bellows pump. The samples were analyzed within 6 months after the cruise at the Rosenstiel School for Marine and Atmospheric Sciences (RSMAS, Miami, Florida) according to Schauffler et al. (1999) with an instrumental precision of ~5 %. Further details ~~on of the precision and the preparation of the samples and the use of standard gases~~ the analysis are described in Montzka et al. (2003) and Fuhlbrügge et al. (2013). On R/A FALCON ambient air was analysed in situ by a GhOST-MS (Gas Chromatograph for the Observation of Stratospheric Tracers – coupled with a Mass Spectrometer) by the Goethe University of Frankfurt (GUF). Additionally 700 ml glass flasks were filled with ambient air to a pressure of 2.5 bar ~~with a diaphragm pump using~~ with the R/A FALCON whole air sampler (WASP) and analysed within 48 hours by a ground-based gas chromatography – mass spectrometry (GC/MS) instrument (Agilent 6973) of the University of East Anglia (Worton et al., 2008). During the flights GhOST measurements were conducted approximately every 5 minutes with a sampling time of 1 minute, while WASP samples were taken every 3 – 15 minutes with a sampling time of 2 minutes. Further details on the instrumental precision and intercalibration ~~of both instruments and observations~~ on R/A FALCON are given in Sala et al. (2014). Given that the ground-based GC/MS investigated only brominated compounds, ~~CH₃I methyl iodide~~ data is not available from WASP. Measurements from R/V SONNE and R/A FALCON were both calibrated ~~both~~ with NOAA standards.

2.3.2. Water samples

~~Sea water samples for dissolved-VSLS~~ sea water samples were taken ~~in-situ on a~~ 3 hourly basis from the moon pool of R/V SONNE at a depth of 5 m from a continuously working water pump. Measurements were interrupted between November 16, 00 UTC to November 17, 2011 12 UTC due to permission issues in the southwest South China Sea. ~~For the analysis~~ The of the water samples were analysed on board with a purge and trap system ~~was,~~ attached to a gas chromatograph with mass spectrometric detection in single-ion mode ~~with~~ and a precision of 10 % determined from duplicates. The ~~approach-method~~ is described in detail by Hepach et al. (2014)

2.3.3. Sea – air flux

The sea – air flux (F) of ~~CHBr₃bromoform,~~ ~~CH₂Br₂dibromomethane~~ and ~~CH₃I methyl-iodide~~ is calculated with k_w ~~as specific transfer coefficient of the compound~~ the concentration gradient, and Δc ~~as the concentration gradient between~~ the specific the water and atmospheric equilibrium concentrations (Eq. 1). For the determination of k_w , ~~the air – sea gas exchange~~ the wind speed-based parameterization of Nightingale et al. (2000) was used and a Schmidt number (Sc) correction to the carbon dioxide derived transfer coefficient k_{CO_2} after Quack and Wallace (2003) was applied for the three gases (Eq. 2).

$$F = k_w \cdot \Delta c \quad (\text{Eq. 1})$$

$$k_w = k_{CO_2} \cdot \frac{Sc^{-\frac{1}{2}}}{600} \quad (\text{Eq. 2})$$

Details on ~~deriving-measuring~~ the air – sea concentration gradient are further described in Hepach et al. (2014) and references therein.

2.4. Oceanic VSLS contribution to the MABL and FT

2.4.1. Trajectory calculations

~~For the determination of the~~ The air mass transport from the surface to the FT was calculated with the Lagrangian Particle Dispersion Model FLEXPART ~~of from~~ the Norwegian Institute for Air Research in the Department of Atmospheric and Climate Research (Stohl et al., 2005) ~~was-used~~. The model has been extensively evaluated in earlier studies (Stohl et al., 1998; Stohl and Trickl, 1999) and includes parameterizations for turbulence in the

atmospheric boundary layer and the FT as well as moist convection (Stohl and Thomson, 1999; Forster et al., 2007). Meteorological input fields are retrieved from the ECMWF (European Centre for Medium-Range Weather Forecasts) assimilation reanalysis product ERA-Interim (Dee et al., 2011) with a horizontal resolution of $1^\circ \times 1^\circ$ and 60 vertical model levels. The ship-based 6 hourly radiosonde measurements (~~Section 2.2.1~~) were assimilated into the ERA-Interim data (~~Section 2.2.1~~) and ~~the 6 hourly input fields~~ provide air temperature, horizontal and vertical wind, boundary layer height, specific humidity, as well as convective and large scale precipitation. For the trajectory analysis, 80 release points were defined along the cruise track. Time and position of these release events are synchronized with the water and air samples (Section ~~2.3.2.3~~). At ~~these each releases event~~, 10,000 trajectories were launched ~~per release point~~ from the ocean surface within a time frame of ± 30 minutes and an area of $\sim 400 \text{ m}^2$.

2.4.2. VSLs source-loss estimate in the MABL

The time scales of air mass transport derived from FLEXPART together with the oceanic emissions and chemical losses of the VSLs are used for a mass balance source-loss estimate over the South China and Sulu Seas ~~is obtained by applying the mass balance principle to the oceanic emissions, and to the time scales of air mass transport from FLEXPART and chemical loss~~. For each release event, ~~we define~~ a box ~~of the size~~ given by the in-situ height of the MABL and by the horizontal area of the trajectory releases ($\sim 400 \text{ m}^2$ centred on the measurement location) is defined. The MABL source-loss estimate is based on the assumption of a constant VSL S mixing ratio (given by the atmospheric measurements), a constant sea – air flux, the chemical loss rate, and a VSLs homogeneous distribution with the box during each release. ~~The MABL source-loss estimate is based on a steady state the assumption of a constant VSLs mixing ratio (given by the atmospheric measurements) and a constant sea to air flux and loss and their homogeneous distribution within these boxes within this box during each release. The average VSLs delivery and loss calculated for these boxes is denoted as MABL source-loss estimate in this manuscript.~~

~~To derive the amount of VSLs delivery to the MABL by oceanic emissions, we consider the specific sea – air flux constant during each trajectory release and the emissions homogeneously distributed in the MABL. The contribution of the sea – air flux to the MABL concentrations of the specific compounds is defined as the Oceanic Delivery (OD). The Oceanic Delivery (OD) is given calculated as the ratio of as the contribution of VSLs sea – air flux flux out of the ocean (in mol per day) and to the total amount of the VSLs in the box~~

(in mol) in percentage per day. ~~with the latter derived from the box dimensions and the measured VSLs mixing ratio, given in percentage per day. Another important process determining the VSLs concentrations in the MABL is the~~ The loss of MABL air to the FT caused by vertical transport, ~~defined denoted~~ here as Convective Loss (*COL*). ~~This loss process~~, is calculated from the mean residence time of the FLEXPART trajectories in the observed MABL during each release and is given as a negative number in percentage per day. ~~and COL equals the loss of VSLs from the MABL to the FT. The Chemical Loss (CL), in the form of reaction with OH and photolysis, is estimated in percentage per day (negative quantity) and is given as a negative quantity Chemical loss processes in form of reaction with OH and photolysis can be described by the chemical lifetime of the VSLs in the MABL. Based~~ based on the tropical MABL lifetime estimates of ~~16-15~~ days for ~~CHBr₃~~ bromoform, ~~60~~ 94 days for ~~CH₂Br₂~~ dibromomethane (Hossaini et al., 2010) and ~~3-4~~ days for ~~CH₃I~~ methyl iodide (R. Hossaini, personal communication) (Carpenter et al., 2014). ~~the Chemical Loss (CL) is estimated in percentage per day and given as a negative quantity.~~

Relating the delivery of VSLs from the ocean to the MABL (*OD*) and the loss of MABL air ~~with the contained~~ containing VSLs to the FT (*COL*) results in an Oceanic Delivery Ratio (*ODR*) (Eq. 3):

$$ODR = \frac{OD [\%d^{-1}]}{-COL [\%d^{-1}]} = \frac{Sea-Air\ flux\ contribution\ [\%d^{-1}]}{Loss\ of\ MABL\ air\ to\ the\ FT\ [\%d^{-1}]} \quad (Eq. 3)$$

Similarly, ~~we relate~~ the Chemical Loss in the MABL (*CL*) ~~related~~ to the MABL VSLs loss into the FT (*COL*) ~~to derives~~ leads to a Chemical Loss Ratio (*CLR*) (Eq. 4):

$$CLR = \frac{CL [\%d^{-1}]}{-COL [\%d^{-1}]} = \frac{Loss\ through\ chemistry\ [\%d^{-1}]}{Loss\ of\ MABL\ air\ to\ the\ FT\ [\%d^{-1}]} \quad (Eq. 4)$$

~~Assuming steady state in the box~~ The oceanic delivery, chemical loss and loss to the FT must be balanced by advective transport of air masses in and out of the box. We define the change of the VSLs through advective transport as Advective Delivery (*AD*) in percentage per day (Eq. 5). Additionally, we define the ratio of change in VSLs caused by advection (*AD*) to the loss of VSLs out of the MABL to the FT as Advective Delivery Ratio (*ADR*) in Eq. 6:

$$AD = -COL - CL - OD \quad (Eq. 5)$$

$$ADR = \frac{AD [\%d^{-1}]}{-COL [\%d^{-1}]} = 1 - CLR - ODR \quad (\text{Eq. 6})$$

Note that for the VSLS within the MABL box, *COL* and *CL* are loss processes and given as negative numbers while *OD* and *AD* (besides very few exceptions for the latter) are source processes and given as positive numbers. In order to derive the ratios, we divided *CL*, *OD* and *AD* by $-COL$ and therefore end up with negative ratios for the loss process and positive ratios for the source processes.

In a final step, we relate the source-loss ratios (*ODR*, *CLR* and *ADR*) to the MABL VSLS volume mixing ratio (VMR_{MABL}) in the box (Eq. 7 – 9), in order to derive-estimate information on newly-supplied VSLS newly supplied results from oceanic delivery (VMR_{ODR}), how much is destroyed-by-lost by chemical processes (VMR_{CLR}) and how much results from-supplied by advective transport (VMR_{ADR}).the different contributions to the observed mixing ratio. Assuming steady state in the box and a complete loss of all air masses into the FT, we want to estimate how much of

$$VMR_{ODR} = ODR \cdot VMR_{MABL} \quad (\text{Eq. 7})$$

$$VMR_{CLR} = CLR \cdot VMR_{MABL} \quad (\text{Eq. 8})$$

$$VMR_{ADR} = ADR \cdot VMR_{MABL} \quad (\text{Eq. 9})$$

2.4.3. Oceanic and MABL VSLS contribution to the FT

~~The cruise covered heterogeneous oceanic regions in the South China Sea.~~ We use a simplified approach to calculate the mean contribution of boundary layer air masses observed from various oceanic regions in the South China Sea on the ship, and the oceanic compounds therein, to the FT above the South China and Sulu Seas. The contribution is determined as a function of time and altitude based on the distribution of the trajectories released at each measurement location along the ship track. According to R/A FALCON observations and our trajectory calculations we assume a well-mixed FT within 5° S - 20° N, 100° E – 125° E. Observations on R/V SONNE, on the other hand, are characterized by large variability and are considered to be representative for the area along the cruise track where the VSLS were measured in the water and atmosphere. We constrain our calculations to this area and define 80 vertical columns along the cruise track. Each column extends horizontally over the area given by the starting points of the trajectories (20 m x 20 m centred on the measurement location) and vertically from the sea surface up to the highest point of R/A FALCON

observations around 13 km altitude. For each of the 80 ~~trajectory releases~~ columns along the cruise track, 10,000 trajectories were launched and assigned an identical MABL air parcel containing air with the VSLs mixing ratios observed on R/V SONNE during the time of the trajectory release. The volume of the air parcel is given by the in-situ height of the MABL and the horizontal extent of the release box (20 m x 20 m) divided by 10,000 trajectories. The transport of the MABL air parcels is specified by the trajectories, assuming that no mixing occurs between the parcels during the transport. Chemical loss of the VSLs in each air parcel is taken into account through chemical degradation according to their specific tropospheric lifetimes. ~~We average over the volume and mixing ratios of all trajectories within the South China Sea area independent of their exact horizontal location. Since t~~ The VSLs mixing ratios in the FT from the aircraft measurements are **considered** representative for the whole South China Sea area, ~~it is for our approach not important where the air parcels reside within this area. Only if trajectories leave the South China Sea area they are not taken into account any longer.~~ Thus we average over the volume and mixing ratios of all trajectories within the **South China Sea area, independent of their exact horizontal location**. Due to the decreasing density of air in the atmosphere with height, the volume of the MABL air parcels expands along the trajectories with increasing altitude. The expanding MABL air parcels take up an increasing fraction of air within the FT column, which is taken into account in our calculations using density profiles from our radiosonde measurements.

We calculate the contribution of oceanic compounds to the FT for 25 layers of 500 m height intervals, ~~situated~~ between 0.5 km and 13 km altitude within the column above the measurement location. For each layer, the ratio r_{MABL} of the volume of the MABL air parcels with the VSLs mixing ratio VMR_{MABL} to the whole air volume of the layer is calculated. The ratio of advected FT air with a mixing ratio VMR_{AFT} to the whole air volume of the layer is r_{AFT} , respectively, with $r_{MABL} + r_{AFT} = 1$. In our simulation, the FT air with a mixing ratio VMR_{FT} observed by R/A FALCON at a specific height is composed of the MABL air parcels and of the advected FT air parcels (Eq. 10):

$$r_{MABL} \cdot VMR_{MABL} + r_{AFT} \cdot VMR_{AFT} = (r_{MABL} + r_{AFT}) \cdot VMR_{FT} \quad (\text{Eq. 10})$$

The relative contribution C_{MABL} of VSLs observed in the MABL to the VSLs observed in the FT is computed in altitude steps of 500 m (Eq. 11):

$$C_{MABL}[\%] = 100 \cdot (r_{MABL} \cdot VMR_{MABL})/VMR_{FT} \quad (\text{Eq. 11})$$

The oceanic contribution C_{ODR} of the South China Sea emissions to the ~~atmospheric mixing ratios~~ VSLS in the FT is computed after Eq. 12:

$$C_{ODR}[\%] = 100pu r_{MABL} \cdot VMR_{ODR}/VMR_{FT} \quad (\text{Eq. 12})$$

The simplified approach also allows ~~us to derive~~ deriving mean VSLS mixing ratios accumulated in the FT from both MABL VSLS and oceanic emissions. The FT VSLS mixing ratios are simulated for each of the 80 ~~releases~~ columns by initiating a new trajectory release event using same meteorological conditions and VSLS MABL observations, when the former MABL air has been transported into the FT, according to the specific residence time in the MABL. The initial FT background mixing ratios are 0 ppt for each VSLS. The accumulated mean mixing ratio of a compound at a specific height is then computed after Eq. 13:

$$VMR_{MFT} = r_{MABL_1} \cdot VMR_{MABL_1} + r_{MABL_2} \cdot VMR_{MABL_2} + \dots + r_{MABL_i} \cdot VMR_{MABL_i} \quad (\text{Eq. 13})$$

Here, VMR_{MFT} is the modelled accumulated FT mixing ratio, r_{MABL_i} is the ratio of MABL air parcels in 20 m x 20 m x 500 m layers between 0.5 km and 13 km altitude to the total volume of each layer, VMR_{MABL_i} is the mixing ratio in the MABL air parcels including chemical degradation since release from the MABL, and i is the number of initiated runs per release. A steady state for the compounds is reached, when variations in their mixing ratios vary less than 1 % between two initiated runs. For CHBr_3 ~~bromoform~~ the steady state is reached after 11.0 ± 2.1 d (mean $\pm \sigma$), 11.8 ± 2.4 d for CH_2Br_2 ~~dibromomethane~~ and 8.0 ± 1.4 d for CH_3I ~~methyl iodide~~. The modelled overall mean FT mixing ratio in the South China Sea is derived as the mean from the 80 individually calculated FT mixing ratios determined along the cruise ~~(Figure xx)~~. The oceanic contribution to the FT compounds is calculated with VMR_{ODR} from Eq. 7 inserted as VMR_{MABL} in Eq. 13.

3. Meteorological conditions in the MABL and the FT

3.1. Meteorology along the ship cruise

Moderate to fresh trade winds ~~are were~~ dominating the South China and Sulu Seas during the cruise (Figure 1 ~~Figure 1a-b~~), ~~which is reflected~~ indicated by the overall mean wind direction

of northeast ($50^\circ - 60^\circ$) and a mean wind speed of $5.5 \pm 2.9 \text{ ms}^{-1}$ ~~during the cruise~~. The wind observations reveal two different air mass origins. Between November 15 and 19, 2011 a gentle mean wind speed of $3.7 \pm 1.8 \text{ ms}^{-1}$ with a *northern* wind direction was observed, influenced by a weak low pressure system (not shown here) over the central South China Sea moving southwest and passing the ship position on 17.11.2011. During November 20 – 29, 2011 the wind direction changed to *northeast* and the mean wind speed increased to moderate $6.4 \pm 3.0 \text{ ms}^{-1}$. A comparison between 6 hourly ERA-Interim wind and a 6 hourly averaged mean of the observed wind on R/V SONNE reveals an underestimation of the wind speed by ERA-Interim along the cruise track by $1.6 \pm 1.4 \text{ ms}^{-1}$ on average (not shown here). The mean deviation of the wind direction between reanalysis and observation is 2 ± 37 degree. Reanalysis and observed wind speeds correlate with $R = 0.76$ and the wind directions with $R = 0.86$, reflecting a good overall agreement between ship observation and ERA-Interim winds. With an observed mean surface air temperature (SAT) of $28.2 \pm 0.8^\circ\text{C}$ and a mean SST of $29.1 \pm 0.5^\circ\text{C}$ the SAT is on average $1.0 \pm 0.7^\circ\text{C}$ below the SST, which benefits convection of surface air (Figure 2~~Figure-2~~). ~~The mean convective-available-potential-energy (CAPE) computed from the radiosonde data is $998 \pm 630 \text{ Jkg}^{-1}$, which benefits convection of surface air.~~ Indeed enhanced convective activity and pronounced precipitation events have been observed during the cruise (S-Figure 14). Figure 3~~Figure-3~~a shows the time series of the relative humidity measured by the radiosondes launched on R/V SONNE from the surface up to the mean height of the cold point tropopause at 17 km. ~~Increased relative humidity within the lower troposphere coincides with the rain fall events observed by the disdrometer on November 16, 21 and 24, 2011. (compare with Figure 3).~~ Elevated humidity is found on average up to about 6 km, which implies a distinct transport of water vapour to the mid troposphere during the cruise by deep convection or advection of humid air from a nearby convective cell.

3.2. Marine atmospheric boundary layer

Higher SSTs than SATs (Figure 2~~Figure-2~~) cause unstable atmospheric conditions (negative values) between the surface and about 50 – 100 m height (Figure 3~~Figure-3~~b). Surface air is heated by warmer surface waters and is enriched with humidity both benefiting moist convection. The stability of the atmosphere increases above $420 \pm 120 \text{ m}$ and indicates the upper limit of the MABL at this altitude range derived from radiosonde data (Figure 3~~Figure-3~~b). The ~~ERA-Interim~~ MABL height given by ERA-Interim along the cruise track is with $560 \pm 130 \text{ m}$ systematically higher (not shown), but still within the upper range of the MABL

height derived from the radiosonde measurements. The unstable conditions of the MABL and the increase of the atmospheric stability above the MABL reflect the characteristics of a convective, well-ventilated tropical boundary layer. In contrast to cold oceanic upwelling regions with a stable and isolated MABL (Fuhlbrügge et al., 2013; Fuhlbrügge et al., 2015), the vertical gradient of the relative humidity measured by the radiosondes (Section 3.1.3.4) and the height of the MABL do not coincide. This is caused by increased mixing through and above the MABL by turbulence and convection, which leads to the convective, well-ventilated MABL.

4. Atmospheric VSLS over the South China and Sulu Seas

4.1. Atmospheric surface observations on R/V SONNE

Overall, the three VSLS show a joint pattern of atmospheric mixing ratios along the cruise track with lower atmospheric surface abundances before 21 November 2011 and higher concentrations afterwards, which can be attributed to a change in air mass origin. Overall, the three VSLS bromoform, dibromomethane and methyl iodide show a similar pattern of atmospheric mixing ratios (Figure 6a) along the cruise track with lower atmospheric surface abundances before November 21, 2011, west of Brunei and higher afterwards, which can be attributed to a change in air mass origin as well as an increase of the observed wind speed (Figure 1 Figure 1). A decrease from 3.4 ppt to 1.2 ppt of CHBr_3 bromoform is found occurs at the beginning of the cruise (Figure 4 Figure 4a) when the ship left Singapore and the coast of the Malaysian Peninsula. On November 16 – 19, 2011, when the ship passed the southern South China Sea, lower mixing ratios (\pm standard deviation 1σ) of 1.2 ± 0.3 ppt prevail and also the lowest mixing ratios for CHBr_3 bromoform during the whole cruise of 0.8 ppt are found observed. At the coast of Borneo and the Philippines, the average mixing ratio of CHBr_3 bromoform increases to 2.3 ± 1.4 ppt. During the two 24 h stations, the mean mixing ratios are 1.4 ± 0.2 ppt for the first and 2.6 ± 0.4 ppt for the second station. The overall mean CHBr_3 bromoform mixing ratio during the cruise is 2.1 ± 1.4 ppt (Table 1 Table 1) and therefore higher than earlier reported CHBr_3 bromoform observations of 1.2 ppt in January – March 1994 (Yokouchi et al., 1997), 1.1 ppt in September 1994 (Quack and Suess, 1999) and 1.5 ppt in June – July 2009 (Nadzir et al., 2014) further offshore in the South China Sea. The higher atmospheric mixing ratios during the R/V SONNE cruise in November 2011 in contrast to the lower mixing ratios in these previous studies may point to stronger local sources, strong seasonal or interannual variations, or even to long-term changes. CH_2Br_2 Dibromomethane shows a mean mixing ratio of 1.2 ± 0.2 ppt (Table 1 Table 1).

Yokouchi et al. (1997) observed a lower mean atmospheric mixing ratio of 0.8 ppt and Nadzir et al. (2014) of 1.0 ppt in the South China Sea. An increase of the CH_2Br_2 dibromomethane mixing ratios from 1.0 ± 0.1 ppt to 1.3 ± 0.2 ppt is observed after November 21, 2011 coinciding with an increase of the CH_3I methyl iodide concentrations from primarily 0.3 ± 0.0 ppt to 0.4 ± 0.1 ppt (Figure 4a). The highest mixing ratio of CH_3I methyl iodide was detected in the south-western Sulu Sea on November 25, 2011 with 0.8 ppt. The overall mean atmospheric mixing ratio for CH_3I methyl iodide, of 0.4 ± 0.1 ppt (Table 1) is lower than the mean of 0.6 ppt observed by Yokouchi et al. (1997). The concentration ratio of CH_2Br_2 dibromomethane and CHBr_3 bromoform (Figure 4b) has been used as an indicator of relative distance to the oceanic source for the age of air masses, after they crossed strong coastal source regions, where a ratio of approximately 0.1 was observed crossing strong coastal source regions (Yokouchi et al., 2005; Carpenter et al., 2003). The ten times elevated CHBr_3 bromoform has a much shorter lifetime, thus degrading more rapidly than CH_2Br_2 dibromomethane, which increases the ratio during transport. Overall, the mean concentration ratio of CH_2Br_2 dibromomethane and CHBr_3 bromoform is 0.6 ± 0.2 , which suggests that predominantly older air masses are advected over the South China Sea. The highest concentration ratio of 1.2, likely indicating the oldest air mass, is observed on November 16, 2011.

4.2. Oceanic surface concentrations and emissions from R/V SONNE

VSLs in the surface sea water along the cruise track show highly variable distributions (Figure 4c and Table 1). Oceanic CHBr_3 bromoform surface concentrations range from $2.8 - 136.9 \text{ pmol L}^{-1}$ with a mean of 19.9 pmol L^{-1} during the cruise, while CH_2Br_2 dibromomethane concentrations range from $2.4 - 21.8 \text{ pmol L}^{-1}$ with a mean of 5.0 pmol L^{-1} . CHBr_3 bromoform and CH_2Br_2 dibromomethane have similar distribution patterns in the sampling region with near shore areas showing typically elevated concentrations. CH_3I methyl iodide concentrations range from $0.6 - 18.8 \text{ pmol L}^{-1}$ with a mean of 3.8 pmol L^{-1} and show a different distribution along the ship track which might be ascribed to additional photochemical production of CH_3I in the surface waters (e.g. Manley and Dastoor, 1988; Manley and de la Cuesta, 1997; Richter and Wallace, 2004) than the two bromocarbons, indicating different sources.

High levels of all VSLs are found in waters close to the Malaysian Peninsula, especially in the Singapore Strait on November 16, 2011, likely possibly showing an anthropogenic influence on the VSLs concentrations. VSLs concentrations decrease rapidly when the cruise

track leads to open ocean waters. Along the west coast (November 19 - 23, 2011) and north east coast of Borneo (November 25, 2011), bromocarbon concentrations are elevated, and especially CHBr_3 concentrations increase in waters with lower salinities, indicating an influence by river run off. Elevated CHBr_3 concentrations are often found close to coasts with riverine inputs caused by natural sources and industrial and municipal effluents (see Quack and Wallace, 2003; Fuhlbrügge et al., 2013 and references therein).

Oceanic emissions were calculated from synchronized measurements of sea water concentrations and atmospheric mixing ratios, sea surface temperatures and wind speeds, measured on the ship (Section 2.3.3.3). The overall VLS distribution along the ship track is opposite for the oceanic and atmospheric measurements (Figure 4a-d). While the sea water concentrations of VLS generally decrease towards the Sulu Sea, the atmospheric mixing ratios increase, leading to a generally lower concentration gradient of the compounds between sea water and air in the Sulu Sea (not shown here).

Coinciding low VLS atmospheric background concentrations, high SSTs, elevated oceanic VLS concentrations and high wind speeds, lead to high emissions of VLS for the South China and Sulu Seas (Figure 4d) of $1486 \pm 1718 \text{ pmol m}^{-2} \text{ h}^{-1}$ for CHBr_3 , $405 \pm 349 \text{ pmol m}^{-2} \text{ h}^{-1}$ for CH_2Br_2 and $433 \pm 482 \text{ pmol m}^{-2} \text{ h}^{-1}$ for CH_3I . In particular, CHBr_3 fluxes are very high and in agreement with thus confirm elevated coastal fluxes from previous campaigns in tropical source regions (Quack et al., 2007). They often exceed $2000 \text{ pmol m}^{-2} \text{ hr}^{-1}$ in the coastal areas and are even reach more sometimes higher than $6000 \text{ pmol m}^{-2} \text{ hr}^{-1}$, as in the Singapore Strait on November 15, 2011 and on November 22, 2011 at the northwest coast of Borneo, which was also an area of strong convection (Figures 1, 4b).

4.3. VLS intercomparison: R/A FALCON and R/V SONNE

The two profiles of the bromocarbon mixing ratios and the profile for CH_3I from the surface to 13 km altitude as observed on R/A FALCON with the GhOST and WASP instruments (Sala et al., 2014; Tegtmeier et al., 2013) and the profile for methyl iodide as observed on R/A FALCON with the GhOST and WASP instruments are shown in Figure 5. Mean CHBr_3 mixing ratios are 1.43 ppt (GhOST) and 1.90 ppt (WASP) in the MABL (0 – 450 m, determined from meteorological aircraft observations similarly as for the radiosondes, Section 2.2.2.2) and 0.56 ppt (GhOST) and 1.17 ppt (WASP) in the FT (0.45 km – 13 km, Table 1). The GhOST mixing ratios in the MABL are considerably lower than those observed on R/V SONNE (2.08 ppt), but higher than the mixing ratios

(Yokouchi et al., 1997) observed by Yokouchi et al. in January to March 1994, by Quack and Suess (1999) in September 1994 and Nadzir et al. (2014) in June/July 2009 at coastal areas. Open ocean observations of Nadzir et al. (2014) with 1.5 ppt are comparable to GhOST, but lower than WASP observations. A very good agreement of the measurements is given for the longer lived CH_2Br_2 dibromomethane with 1.17 ppt (R/V SONNE), 1.19 ppt (GhOST) and 1.15 ppt (WASP). CH_3I methyl iodide mixing ratios measured by GhOST are 0.59 ± 0.30 ppt within the MABL of 450 m height, which is about 0.2 ppt higher than the values from R/V SONNE, but coincide with the observations by Yokouchi et al. (1997). Above the MABL, the average mixing ratio of CH_3I methyl iodide decreases to 0.26 ± 0.11 ppt (Figure 5 Figure 5). CHBr_3 bromoform and CH_2Br_2 dibromomethane concentrations of all instruments in the MABL correlate with $R = 0.83$ for all instruments (Figure 6 Figure 6). CHBr_3 bromoform and CH_3I methyl iodide concentrations correlate with $R = 0.55$ and CH_2Br_2 dibromomethane and CH_3I methyl iodide with $R = 0.66$; all three correlations are significant at 99 %. Even higher correlations are found if only measurements on R/V SONNE are taken into account with $R = 0.92$ for CHBr_3 bromoform and CH_2Br_2 dibromomethane, $R = 0.64$ for CHBr_3 bromoform and CH_3I methyl iodide, and $R = 0.77$ for CH_2Br_2 dibromomethane and CH_3I methyl iodide. Two case studies for the Comparison of R/A FALCON and R/V SONNE data are obtained from their meetings on November, 19 and 21, 2011 (Table 2 Table 2), when aircraft and ship passed each other within 100 m distance several times, measuring the same air masses. During both meetings, deviations between the GhOST and WASP instruments on the aircraft are larger for the bromocarbons than the deviation between the WASP and the ship measurements. According to Sala et al. (2014) the agreement between the GhOST and WASP instruments are within the expected uncertainty range of both instruments which is then assumed to be also valid for the ship measurements (this study). The good agreement between WASP and ship data might be caused by the same sampling and analysis method, both using stainless steel canisters and subsequent analysis with GC/MS, while GhOST measures in-situ with a different resolution. WASP and the ship data, which agree very well, rely on sampling of air in stainless steel canisters and subsequent analysis with GC/MS while GhOST measures in-situ. Since GhOST and WASP measurements together cover a larger spatial area and higher temporal resolution, a mean of both measurements is used in the following for computations in the free troposphere. For CH_3I significantly higher mixing ratios were measured during the meetings between ship and aircraft (Table 2 Table 2). Whether this offset is systematic for the different methods, needs to be investigated further

investigation. The methyl iodide values of the GhOST and air canister data from the ship show larger differences during the second meeting.

In the following, a mean of the GhOST and WASP measurements of R/A FALCON is used for computations in the free troposphere.

5. Air mass and VLS transport from the surface to the free troposphere

5.1. Timescales and intensity of vertical transport

Forward trajectories have been computed with FLEXPART starting at sea level along the cruise track between Singapore to Manila. ERA-Interim is used for the meteorological input (Section 2.2.1). The FLEXPART runs, yield an average MABL residence time of 7.8 ± 3.5 hours before the trajectories enter the FT (Figure 7), reflecting a relatively fast exchange due to the convective well ventilated MABL (Figure 3). The trajectories generally show a strong contribution of surface air masses to the FT, despite some exceptions during November 18 – 22, 2011 (Figure 7). The trajectories furthermore reveal a very Most intense and rapid transport of MABL air masses up to 13 km height occurs within 2–3 days on November 17 and 23, 2011. To estimate the loss of air masses out of the South China Sea area between 5° S – 20° N and 100° E – 125° E (Section 2.4.3) we determine the loss of trajectories out of this area after their release (Figure 8). After 4 days, 88 % of all trajectories released along the cruise track are still within this defined area of the South China Sea, which decreases to and 31 % after 10 days. During these ten days 65.1 ± 22.2 % of the trajectories have passed 6 km height and 20.4 ± 9.7 % have passed 13 km height within the area, while 18.5 % of the trajectories re-enter the MABL from the FT. Most intense convection within FLEXPART calculations along the cruise track occurred on November 17 and 18, 2011 in the southern South China Sea (Figure 9), November 22–24 at the north western coast of Borneo and on November 25–26 in the Sulu Sea. 30–50 % of the trajectories released from the surface at these times ascend to 13 km height within 3–4 days. Discrepancies to CAPE observations on R/V SONNE (Figure 3) are due to the fact that the calculated CAPE describes the stability of the air column that is observed by the radiosondes ascending with weather balloons, while the trajectories simulate the actual movement of the air masses, thus include the convection in other regions after some hours of transport time. Indeed during convective events at the northern coast of Borneo, the majority of trajectories were transported south towards the coast of Borneo where active convection took part. Trajectories launched between November 18–22 during 0 and 12 UTC each day reveal a longer residence time of up to 5 days in the lower troposphere (Figure 9). At about 2 km

altitude a barrier seems to suppress convection during this time. This agrees with our CAPE observations, showing suppressed convection at about 1.5 km altitude north of Borneo (Figure 3), as lowest observed CAPE is predominantly found between 0 and 12 UTC during these days.

5.1.1.1.1. R/V SONNE – R/A FALCON: Identifying observations of the same air mass

To investigate if the same air masses were observed on R/V SONNE and on R/A FALCON a perfluorocarbon tracer was released on R/V SONNE on November 21, 2011, which was indeed detected 25 hours later on R/A FALCON (Ren et al., 2014). With the trajectory calculations it can be determined which fraction of the air masses investigated on R/V SONNE could subsequently be investigated on R/A FALCON. Within a horizontal distance of ± 20 km and a maximum vertical distance of ± 1 km around the position of the aircraft, as well as a time frame of ± 3 hrs of the VSLS air measurements on R/A FALCON, 15 % of all launched 80 x 10,000 surface trajectories, marking the air masses on R/V SONNE, passed the R/A FALCON flight track during the cruise. Allowing a time frame up to 10 days, the amount of trajectories passing the flight track of R/A FALCON increases to 77 ± 29 % between November 16 and December 11, 2011. In the following we combine the R/V SONNE and R/A FALCON measurements to derive the contribution of oceanic VSLS to MABL and FT concentrations based on the observations.

5.2. Contribution of oceanic emissions to VSLS in the MABL

From the sea – air fluxes (Section 4.2) and the residence times of the surface trajectories in the MABL (Section 5.1), the Oceanic Delivery (OD) and the CONvective Loss (COL) were computed (Table 3) using the method described in Section 2.4.2.

The contribution of the flux to the observed atmospheric VSLS concentration in the MABL (Oceanic Delivery, OD), whose height is determined from the radiosondes, is scaled to 1 day (Table 3, Figure 11). The OD is 116.4 ± 163.6 % per day to the MABL concentrations for bromoform, 54.2 ± 66.7 % d^{-1} for dibromomethane and 166.5 ± 185.8 % d^{-1} for methyl iodide. In other words, the oceanic source for bromoform is strong enough to fill up the MABL above the measurement location on average about once per day, while for dibromomethane the emissions are weaker and nearly 2 days would be required until the observed mixing ratios in the MABL are reached. Based on the FLEXPART trajectories, the mean loss of MABL air to the FT during one day (CONvective Loss, COL) is computed to be

~~-307.6 ± 124.3 % d⁺. According to the MABL lifetimes of the VSLS the loss due to~~
~~photolysis and OH, both defined as Chemical Loss (CL) in the MABL is 6.6 % d⁺ for~~
~~bromoform, 1.8 % d⁺ for dibromomethane and 30.7 % d⁺ for methyl iodide. In order to~~
~~balance the delivery from the ocean and the loss to the FT and by chemical degradation, an~~
~~Advective Delivery (AD) of VSLS in and out of the MABL is needed. The AD for~~
~~bromoform is 197.9 ± 199.7 % d⁺, for dibromomethane 255.2 ± 131.9 % d⁺ and for methyl~~
~~iodide 171.8 ± 242.3 % d⁺. The numbers indicate that, approximately twice as much VSLS~~
~~would be advected to reach the MABL mixing ratio, if no OD or COL occurred. OD and AD~~
~~are transported via COL into the FT. Based on the OD and the COL, the Oceanic Delivery~~
Ratio (ODR) is calculated in order to characterize the relative contribution of the local
oceanic emissions compared to the loss of MABL air into the FT (Table 3Table 3, Figure
9Figure 9). The average ODR during the cruise is 0.45 ± 0.55 for CHBr₃bromoform, which
means that the loss from the MABL to the FT is balanced to 45 % by oceanic emissions along
the cruise track. The ODR for CH₂Br₂dibromomethane is 0.20 ± 0.21 and for CH₃I methyl
iodide 0.74 ± 1.05, respectively, suggesting that the major amount of CH₃I methyl iodide
originates from nearby sources. Similarly to the ODR the CL is related to the COL to derive
the Chemical Loss Ratio (CLR) for the VSLS, which is 0.03 ± 0.01 for CHBr₃bromoform,
0.01 ± 0.00 for CH₂Br₂dibromomethane and 0.09 ± 0.04 for CH₃I methyl iodide. When
compared to the other source and loss processes, the chemical loss appears negligible for all
three gases. The ratio of the advective delivery (ADR) relating the AD to the COL is 0.58 ±
0.55 for CHBr₃bromoform, 0.80 ± 0.21 for CH₂Br₂dibromomethane and 0.35 ± 1.02,
implying that most of the observed CH₂Br₂dibromomethane (80 %) in the MABL is advected
from stronger other source regions. Applying the ratios ODR to the observed mixing ratios in
the MABL gives an estimate of the amount of the VSLS that originating from the local
oceanic emissions (VMR_{ODR}, Table 4Table 4) that are degraded chemically (VMR_{CLR}) and
that are advected (VMR_{ADR}, Table 4). The local ocean emits a concentration that equates to
0.89 ± 1.12 ppt CHBr₃bromoform, 0.25 ± 0.26 ppt CH₂Br₂dibromomethane and 0.28 ± 0.40
ppt CH₃I methyl iodide in the MABL. The amount that is destroyed by chemistry in the
MABL before the air is transported into the FT accounts to 0.05 ± 0.04 ppt (bromoform),
0.01 ± 0.01 ppt (dibromomethane) and 0.05 ± 0.03 ppt (methyl iodide). Finally 1.18 ± 1.20
ppt of the observed mixing ratios of bromoform, 0.92 ± 0.27 ppt of dibromomethane and 0.14
± 0.37 ppt of methyl iodide are advected. The average transport from the MABL to the FT
(Flux_{MABL-FT}), computed from the MABL concentrations and the trajectory residence time in
the MABL, is 4240 ± 1889 pmol m⁻² hr⁻¹ for CHBr₃bromoform, 2419 ± 929 pmol m⁻² hr⁻¹ for

CH_2Br_2 ~~dibromomethane~~ and $865 \pm 373 \text{ pmol m}^{-2} \text{ hr}^{-1}$ for CH_3I ~~methyl iodide~~. Calculations with the ERA-Interim MABL height, which is on average 140 m higher than the one derived from the radiosondes ~~derived one~~, leads to very similar estimates (S-Table 11).

Since the wind is a driving factor for oceanic emissions and advection of VSLs, changes in wind speed are assumed to affect atmospheric VSLs mixing ratios in the MABL during this cruise. Significant correlations are found between wind speed and the observed mixing ratios of all three VSLs in the MABL with correlation coefficients of $R = 0.55$ (CHBr_3 ~~bromoform~~), $R = 0.57$ (CH_2Br_2 ~~dibromomethane~~) and $R = 0.56$ (CH_3I ~~methyl iodide~~), respectively. Mixing ratios that originate from oceanic emissions ~~The according amount of mixing ratios that originate from the oceanic emissions~~ (VMR_{ODR}) correlate significantly to the wind speed with $R = 0.52$, $R = 0.72$ and $R = 0.62$, respectively. On the opposite, VMR_{ADR} , which is calculated as the residual from VMR_{ODR} , is negatively correlated to the wind speed with $R = -0.21$, $R = -0.32$ and $R = -0.53$. The correlations reveal that the contribution of oceanic emissions to MABL VSLs increase for higher wind speeds, while the advective contribution decreases.

5.3. Oceanic contribution to the FT

5.3.1. Identification of VSLs MABL air ~~and their contained VSLs~~ in the FT

With a simplified approach (method description in Section 2.4.3 ~~2.4.3~~) we are able to estimate the contribution of MABL air and regional marine sources observed on R/V SONNE to the FT. Individual MABL air masses during the cruise show the strongest contribution to the FT air within the lower 3 km of the atmosphere during the first 6 days after release (Figure 10 ~~Figure 10a-f~~). Once the MABL air is spread in the FT column, a decrease of the contribution with time is ~~contribute on average over 20 % to the lowest FT air right after they leave 0.5 km altitude (Figure 12). Within 2 – 6 days after crossing that level an observed MABL air mass contributes up to 15 % depending on the height. A decrease of the contribution with height down to 3 % occurs until 8 km altitude. Above this height, the contribution of the MABL air masses increases again to over 5 % as a result of the density driven extension of the air parcels. The temporal decrease~~ due to the transport of trajectories out of the predefined South China and Sulu Seas area and their chemical loss (Figure 8 ~~Figure 8~~) ~~is visible after three days~~.

The average contribution of VSLs concentrations ~~from in~~ the MABL air to the FT ~~mixing ratio~~ concentrations (c_{MABL}) is generally highest for CHBr_3 , with about 5 – 10 % above ~~between 2–3 km and 11 km altitude height~~ within 10 days (coloured contours in Figure 10 ~~Figure 10a~~), after release is with 1 – 28 % highest for bromoform followed by 1 – 12 % for

CH_2Br_2 dibromomethane (2 – 5 % Figure 10b) and only 0 – 5.3 % for the short-lived CH_3I methyl iodide (Figure 10c) (coloured contours in Figure 12). For all compounds, the largest contributions of >25 % are found between 0.5 km and 2 km height within the first 2 days after release due to occasional fresh entrainment of MABL air. Above 8 km altitude, the average contribution of the individual MABL VSLs releases increase again to >11 % (bromoform), >5 % (dibromomethane) and >3 % (methyl iodide), due to the density driven extension of the MABL air parcels with height. The chemical degradation of CH_3I methyl iodide, according to its short tropospheric lifetime of 4–3.5 days leads to a rapid decrease of the contribution is visible already 2 days after release, when its contribution decreases to <7 % within 0.5 km – 2.5 km altitude and to <2.5 % above 2.5 km altitude.

To identify the contribution of the oceanic emissions to the FT VSLs during the cruise, the VMR_{ODR} of each compound is used as the initial mixing ratio in the MABL air mass. For CHBr_3 and CH_2Br_2 the local emissions contribute only up to 6 % and 2 % to the FT concentrations (c_{ODR} , Figure 10d-e) compared to the 10 %, respectively 5 %, of c_{MABL} . In contrast, the contribution of the local oceanic emissions of CH_3I (Figure 10f) is almost similar to the contribution of the observed MABL concentrations (Figure 10c). The mean contribution of marine compounds from the South China Sea to the FT air varies with time and altitude, but is generally higher for bromoform with 1 – 13 % than for methyl iodide with 0 – 4 %. This is not surprising, considering the longer lifetime of bromoform compared to methyl iodide, although the relative contribution of oceanic emissions to MABL air (Section 5.2) was identified to be higher for methyl iodide (74 %) than for bromoform (45 %). The low mean regional marine contribution of dibromomethane to the observed MABL mixing ratio of 21 % is also reflected in its mean oceanic contribution of only 0 – 3 % to the FT air masses.

5.3.2. Accumulated VSLs in the free troposphere

By simulating a steady transport of MABL air masses into the FT, mean accumulated VSLs mixing ratios in the FT along and during the cruise were computed (Figure 11) as described in 2.4.3. The simulated FT mixing ratios of CHBr_3 bromoform and CH_2Br_2 dibromomethane from the observed MABL (VMR_{MABL}) decrease on average from 1.7 and 1.1 ppt at 0.5 km height to 0.6 and 0.6 ppt at 7 km height and increase again above 8 km up to 0.8 (CHBr_3 bromoform) and 0.8 ppt (CH_2Br_2 dibromomethane). Simulated CH_3I methyl iodide shows a decrease from 0.20 ppt at 0.5 km to 0.05 ppt at 3 km. Above this

altitude, the simulated mixing ratios of CH_3I methyl iodide are quite-almost constant with 0.05 ppt.

To estimate the accumulated FT mixing ratios solely from oceanic emissions, the VMR_{ODR} is used as the initial MABL mixing ratio (Figure 11Figure 11). The simulated FT mixing ratios using either VMR_{MABL} or VMR_{ODR} as input reveal a similar vertical pattern, since both simulations are based on the same meteorology and trajectories. While FT mixing ratios based on VMR_{MABL} and VMR_{ODR} are similar for CH_3I methyl iodide (due to the large oceanic contribution to the MABL mixing ratios), FT mixing ratios from VMR_{ODR} are on average ~0.5 ppt lower for CHBr_3 bromoform and ~0.6 ppt CH_2Br_2 dibromomethane than from VMR_{MABL} . Comparing the simulated VMR_{MABL} FT mixing ratios with the observed FT mixing ratios from R/A FALCON reveals stronger vertical variations for the simulations in contrast to the observations. CHBr_3 Bromoform is overestimated in the VMR_{MABL} simulation between 0 and 4 km altitude, as well as between 9 km and above 12 km. Simulated CH_2Br_2 dibromomethane in the FT based on VMR_{MABL} underestimates the observed mixing ratios between 6 and 10 km height. In particular, the maximum between 7 and 9 km height is not reflected in the simulations. However, observations of both bromocarbons are within 1σ of the FT simulations with MABL air. The CH_3I methyl iodide simulations show a distinct underestimation of the observed FT mixing ratios. ~~In Section 4.3 we have shown that methyl iodide measured in same air masses by R/V SONNE and R/A FALCON was 51 % higher for the aircraft (Table 2).~~ Adjusting all the R/A FALCON values by this-the identified offset to R/V SONNE (Section 4.3 and Table 2) reveals a better agreement between observed and simulated FT mixing ratios (Figure 11Figure 11).

5.3.3. Discussion

Oceanic emissions of CHBr_3 from the South China Sea contribute on average 60 % to the FT mixing ratios observed on the aircraft, while simulations based on the MABL mixing ratios reflect the observations in the FT quite well. Thus, we assume that the observed MABL mixing ratios of CHBr_3 are representative for the South China and Sulu Seas. In case of CH_2Br_2 the underestimation of simulated FT mixing ratios between 6 and 10 km using observed MABL mixing ratios may be due to higher background concentrations of CH_2Br_2 in the mid to upper troposphere given the long atmospheric lifetime of 150 days at these levels. -On average, 45 % and 20 % of CHBr_3 and CH_2Br_2 abundances, respectively, in the MABL observed by the ship originate from local oceanic emissions along the ship track. Thus advection from stronger source regions, possibly along the coast (for CHBr_3) and from the

West Pacific (CH_2Br_2), are necessary to explain the mixing ratios. ~~The simulations show how local oceanic emissions and advection of remote air can explain the observed FT mixing ratios (Figure 13). Local oceanic emissions of bromoform from the South China Sea contribute about 60% to the FT mixing ratios. However,, while simulations based on the MABL mixing ratios clearly overestimate the observations in the FT. In order to explain the FT bromoform profiles from the aircraft observations, we need to take into account advection from other FT regions within the South China Sea has to be taken into account, which. This FT advection leads to lower bromoform than the convection out of the MABL along the cruise track. The bromoform found in the MABL originates to 45% from local sources along the ship track. Accordingly, advection from stronger source regions, possibly along the coast, is necessary to explain the remaining 55% of the bromoform abundance in the MABL.. The fact that the MABL bromoform observed along the cruise track is too high for the local emissions and also too high for the FT profiles above the South China Sea, suggests that the local MABL observations are impacted by additional stronger source regions and may not be representative for the whole region. Observations of lower atmospheric bromoform mixing ratios by Yokouchi et al. (1997), Quack and Suess (1999) and Nadzir et al. (2014) in the South China Sea (Section 4.1) confirm this assumption.~~

~~Dibromomethane in the FT derived from MABL abundances matches the aircraft observations quite well, indicating that dibromomethane observations in the MABL along the cruise track are representative for the region. While in the FT, advection of air masses with different mixing ratios is not necessary to explain the observed dibromomethane, the situation is reversed in the MABL. Significant advection of dibromomethane rich air is necessary to explain the observations in the MABL, since only low oceanic sources were observed during the cruise. The impact of advection on the dibromomethane mixing ratio is enhanced by its relatively long tropospheric lifetime of 120 days.~~

In contrast to CHBr_3 bromoform and CH_2Br_2 dibromomethane, the simulated mixing ratios of CH_3I methyl iodide in the FT are strongly underestimated no matter whether observed MABL mixing ratios or oceanic emissions are used. ~~Due to its short tropospheric life time of 4 days methyl iodide is rapidly degraded during the transport into the FT.~~ The offset between the simulated and observed FT CH_3I methyl iodide could be caused by additional strong sources of CH_3I methyl iodide in the South China Sea area. Furthermore, modelling or measurement uncertainties may add to this offset, ~~which we all discuss in the following:~~

The simulations use constant atmospheric lifetimes for each compound and neglect variations with altitude which could impact the simulated abundances. However, the altitude variations

of the CH₃I methyl iodide lifetime in the MABL and FT are around 0.5 days (Carpenter et al., 2014) and thus impacts on the simulated abundances are quite small. Therefore it seems unlikely that the lifetime estimate causes a large underestimation of the FT CH₃I methyl iodide. Additional uncertainties may arise from cloud induced effects on photolysis rates (Tie et al., 2003) and OH levels (e.g. Tie et al., 2003; Rex et al., 2014) impacting the VSL lifetimes. ~~Therefore it seems unlikely that the lifetime estimate causes a large underestimation of the FT methyl iodide.~~ Deficiencies in the meteorological input fields and the FLEXPART model, in particular in the boundary layer and in the convection parameterizations would affect all compounds and their contribution to the FT concentrations in a similar way and thus seems to be unlikely as well. Ship and aircraft measurements revealed a possible instrumental offset for CH₃I_s, ~~while observing the same air masses, which is probably cannot be resolved due to the different applied calibration scales~~ (Section 4.3.4.3). When we adjust ~~for a constant factor, by which the~~ observations for the offset of CH₃I methyl iodide in the MABL ~~differed~~ between R/V SONNE and R/A FALCON the simulated and observed FT mixing ratios match better. Thus, an instrumental offset causing, at least partially, the calculated discrepancy for CH₃I methyl iodide appears likely (Section 2.3.12.3.1).

Another explanation for the elevated CH₃I methyl iodide in the FT is advection of fresh air with elevated CH₃I methyl iodide mixing ratios in the FT from e.g. South East Asia or the Philippines. These areas are known to comprise strong sources for atmospheric CH₃I methyl iodide from e.g. rice plantations (Redeker et al., 2003; Lee-Taylor and Redeker, 2005). In combination with convective activity over land, which is common in this area (Hendon and Woodberry, 1993), the high observed FT mixing ratios of CH₃I methyl iodide could be explained, despite the low oceanic contribution during the cruise. The low observed MABL mixing ratios of CH₃I methyl iodide on R/V SONNE may thus also not be representative for the area. Yokouchi et al. (1997) observed higher atmospheric CH₃I methyl iodide mixing ratios in the South China Sea.

Finally, the method of our simplified approach includes uncertainties as well. Different parameterizations for the transfer coefficient k_w such as Liss and Merlivat (1986), which is at the lower end of reported parameterizations, and Wanninkhof and McGillis (1999), which is at the higher end, are discussed in Lennartz et al. (2015). Both lead to a reduction of the oceanic contribution to the atmospheric mixing ratios at the observed average moderate wind speeds (~6 ms⁻¹) when applied to our data. Nonetheless, the general conclusion that local oceanic sources of CHBr₃ and CH₃I significantly contribute to MABL mixing ratios remains

for the cruise. In times of possible higher wind speeds ($>10 \text{ ms}^{-1}$), which are likely for this region, the flux variations between the different parameterizations as well as the oceanic contribution to atmospheric abundances, would increase. Since observational studies quantifying the oceanic contribution to atmospheric abundances of VSLs are quite rare, it is difficult to evaluate our findings at the moment and more studies for different oceanic regimes should be carried out to validate our results.

6. Summary

The contribution of oceanic VSLS emissions to marine atmospheric boundary layer (MABL) and free troposphere (FT) air during the SHIVA campaign in November 2011 in the South China and Sulu Seas was investigated in this study. Meteorological parameters were measured near the ocean surface and in the troposphere by regular radiosonde launches on R/V SONNE during the cruise. Oceanic VSLS emissions were determined from simultaneous atmospheric observations and sea surface water concentrations. The transport from the surface through the MABL into the FT was computed with the trajectory model FLEXPART.

The ship ~~cruise-campaign~~ was dominated by north-easterly winds with a characteristic moderate mean wind speed of 5.5 ms^{-1} . The radiosonde launches revealed ~~the high convective potential of the South China and Sulu Seas with an average convective available potential energy (CAPE) of $998 \pm 629 \text{ J kg}^{-1}$ and~~ a convective, well-ventilated, weakly developed MABL with an average height of $420 \pm 120 \text{ m}$ during the cruise. 800,000 forward trajectories, launched from the ocean surface along the cruise track, show a rapid exchange of MABL air with the FT within 7.8 hrs. ~~This study concentrates on the three very short-lived substances bromoform, dibromomethane and methyl iodide which are known to impact tropospheric and stratospheric ozone. On the one hand,~~ The observations on R/V SONNE reveal high mean ocean surface concentrations and emissions for ~~CHBr₃bromoform~~ ($19.94 \text{ pmol L}^{-1}$ and $1486 \text{ pmol m}^{-2} \text{ hr}^{-1}$), ~~CH₂Br₂dibromomethane~~ (4.99 pmol L^{-1} and $405 \text{ pmol m}^{-2} \text{ hr}^{-1}$) and ~~CH₃I methyl iodide~~ (3.82 pmol L^{-1} and $433 \text{ pmol m}^{-2} \text{ hr}^{-1}$) in comparison to other oceanic source regions. Atmospheric mixing ratios in the MABL, on the other hand, are relatively low ~~compared to earlier campaigns~~ with mean values of 2.08 ppt ~~CHBr₃bromoform~~, 1.17 ppt ~~CH₂Br₂dibromomethane~~, and 0.39 ppt ~~CH₃I methyl iodide~~. The contribution of the oceanic VSLS emissions to their MABL concentrations was evaluated by simple source-loss ~~estimations~~estimates, resulting in an Oceanic Delivery Ratio (ODR). The ODR for ~~CHBr₃bromoform~~ is ~~computed to be~~ 0.45, revealing that up to 45 % of ~~CHBr₃bromoform~~ mixing ratios in the MABL above the marginal seas originated, on

average, ~~to 45%~~ from local oceanic sources. ~~The ODR for~~, while 74 % of CH₃I and only 20 % of CH₂Br₂ ~~dibromomethane is 21% and 74% for of methyl iodide 74% originates from~~ the local ocean. This ~~indicating~~ indicates that the long-lived CH₂Br₂ ~~dibromomethane~~ is largely advected in the MABL, ~~while the short-lived methyl iodide. originates mainly from the local ocean.~~

We extend our analysis to the FT using VSLs ~~profiles obtained from~~ observations ~~on~~ from R/A FALCON above the South China Sea. ~~The average contribution of~~ A single MABL air release ~~to~~ contributes up to 28 % (CHBr₃ ~~bromoform~~), 12 % (CH₂Br₂ ~~dibromomethane~~) and 5 % (CH₃I) ~~methyl iodide~~ to the FT mixing ratio (Section 5.3.1 ~~5.3.1~~) ~~is up to 28% (bromoform), 12% (dibromomethane) and 5% (methyl iodide).~~ The mean contributions of the local oceanic VSLs to the FT within this MABL air release are up to 13 % (CHBr₃ ~~bromoform~~), 3 % (CH₂Br₂ ~~dibromomethane~~) and 4 % (CH₃I ~~methyl iodide~~). In order to estimate if the accumulated contributions from the single MABL air releases ~~is~~ are sufficient to explain the accumulated VSLs mixing ratios observed in the FT, ~~we simulate~~ a steady transport of observed MABL air masses and oceanic emissions into the FT above the South China Sea ~~was simulated~~. The simulations for CHBr₃ ~~bromoform~~ based on the volume mixing ratios in the MABL (VMR_{MABL}) ~~overestimated~~ reflect the ~~observations~~ observed mixing ratios in the FT, while the simulations based on the local oceanic emissions ~~of bromoform from the South China Sea~~ (VMR_{ODR}) explained about 60 % ~~of the observed FT mixing ratio.~~ In the MABL, the local oceanic emissions along the cruise track ~~can~~ also explain half of the CHBr₃ ~~bromoform which is also too high for the FT observations.~~ Thus, we conclude that the observed mixing ratios of CHBr₃ ~~bromoform~~ in the MABL are influenced by stronger, ~~local possibly coastal sources, in the region and may not be representative for the whole South China Sea where we expect generally lower values.~~

CH₂Br₂ ~~Dibromomethane~~ in the FT, simulated from observed MABL mixing ratios, shows a good agreement between observations and simulations. However, slightly lower simulated mixing ratios in the mid to upper troposphere compared to the observations indicate an accumulation of CH₂Br₂ at these levels due to its longer atmospheric lifetime compared to CHBr₃. ~~It is most likely mixed in the FT with advected air masses containing similar dibromomethane mixing ratios.~~ CH₃I ~~Methyl iodide~~ in the FT is ~~strongly~~ underestimated in the simulations, using both the observed MABL mixing ratios and the oceanic emissions. ~~The disagreement points either to~~ Even addressing an unresolved offset between the ship and aircraft data leads to an underestimation of CH₃I in the FT, which points to ~~an underestimation of representative methyl iodide MABL mixing ratios and to~~ additional

CH₃I ~~methyl iodide~~ sources, e.g. rice plantations in the region together with pronounced convection ~~South East Asia that were not covered by the ship cruise.~~

Our investigations show how oceanic emissions of VSLS in a strong oceanic source region contribute to the observed atmospheric mixing ratios in the MABL. Furthermore, the contributions of these atmospheric mixing ratios, and the local oceanic VSLS, to the observed VSLS in the FT above this source region are derived. The results reveal strong links between oceanic emissions, atmospheric mixing ratios, MABL conditions and prevailing convective activity in the troposphere. The methods should be applied to other oceanic regions to derive a better process understanding of the contributions of air-sea gas exchange on atmospheric abundances. For the detection of future climate change effects on ocean surface trace gas emissions and their influence on atmospheric chemistry and composition it is important to study the complex interplay between oceanic sources and emissions, meteorology, atmospheric mixing ratios, and transport to the upper atmosphere.

Supplement

Convective energy and precipitation

Intense solar insolation and high sea surface temperatures (SST) favour the South China and Sulu Seas for high convective activity. To indicate atmospheric instabilities that can lead to convective events the convective available potential energy (CAPE) (Margules, 1905; Moncrieff and Miller, 1976) is calculated. CAPE is defined as the cumulative buoyant energy of an air parcel from the level of free convection (LFC), the level where the environmental temperature decreases faster than the moist adiabatic lapse rate of a saturated air parcel at the same level, and the equilibrium level (EL), the height at which the air parcel has the same temperature as the environment. CAPE is computed after S-Eq. 1, with g as the gravitational constant, $T_{v,p}$ as the virtual temperature of an adiabatic ascending air parcel at geometric height z , $T_{v,e}$ as the virtual temperature of the environment at z , z_{LFC} as the height of the level of free convection and z_{EL} as the height of the equilibrium level. CAPE can range from 0 to more than 3 kJ/kg for very intense thunderstorms (Thompson and Edwards, 2000).

$$CAPE = \int_{z_{LFC}}^{z_{EL}} g \cdot \left(\frac{T_{v,p} - T_{v,e}}{T_{v,e}} \right) dz \quad (\text{S-Eq. 1})$$

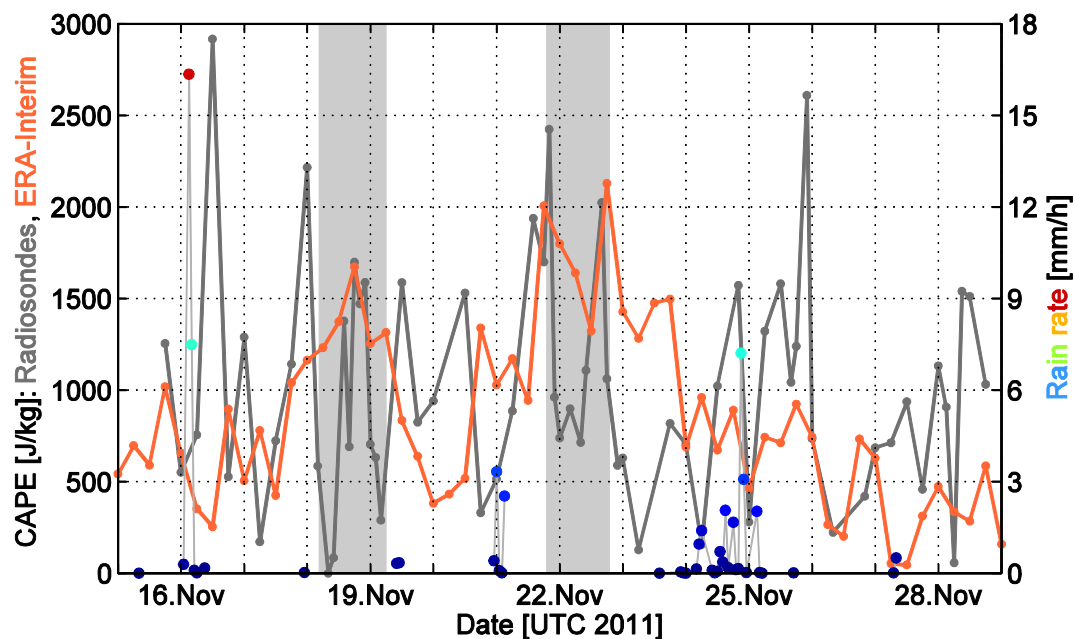
The mean CAPE computed from the radiosonde data is $998 \pm 630 \text{ Jkg}^{-1}$ and typically elevated for tropical regions (S-Figure 1~~4~~). Highest CAPE during the cruise was observed on November 16, 2011 at 12 UTC in the southern South China Sea and exceeded 2.9 kJkg^{-1} , revealing developing convection. ERA-Interim mean CAPE during the cruise was $825 \pm 488 \text{ Jkg}^{-1}$ and about 170 Jkg^{-1} lower than observed by the radiosondes.

Precipitation measurements by the optical disdrometer ODM-470 are shown in S-Figure 1~~4~~. Besides a number of small rain events during the cruise, three major convective rain events are evident on November 16, 21 and 24, 2011. The total amount of accumulated rain during the cruise was 52.3 mm. The most intense rain rate of 16.3 mmh^{-1} was observed on November 16, 2011 in the southwest South China Sea. The relatively low total precipitation during the cruise is reflected by negative precipitation anomalies in November 2011 compared to the long term climate mean along the northern coast of Borneo (Climate Diagnostics Bulletin, November 2011, Climate Prediction Center).

R/V SONNE – R/A FALCON: Identifying observations of the same air mass

To investigate if the same air masses were observed on R/V SONNE and on R/A FALCON a perfluorocarbon tracer was released on R/V SONNE on November 21, 2011, which was indeed detected 25 hours later on R/A FALCON (Ren et al., 2014). With the trajectory calculations it can be determined which fraction of the air masses investigated on R/V SONNE could subsequently be investigated on R/A FALCON. Within a horizontal distance of ± 20 km and a maximum vertical distance of ± 1 km around the position of the aircraft, as well as a time frame of ± 3 hrs of the VSLS air measurements on R/A FALCON, 15 % of all launched 80 x 10,000 surface trajectories, marking the air masses on R/V SONNE, passed the R/A FALCON flight track during the cruise. ~~Allowing a time frame up to 10 days, †~~The amount of trajectories passing the flight track of R/A FALCON increases to 77 ± 29 % between November 16 and December 11, 2011 within a time frame of up to 10 days. ~~In the following we combine the R/V SONNE and R/A FALCON measurements to derive the contribution of oceanic VSLS to MABL and FT concentrations based on the observations.~~

1465



1466

1467

S-Figure 1:

1468

Figure 3:-Left scale: convective available potential energy (CAPE) from radiosondes on R/V SONNE (grey) and ERA-Interim (orange). Right scale: Rain rate (colored dots) during the
cruise, observed by an optical disdrometer (ODM 470) on R/V SONNE. The two shaded
areas (light grey) in the background show the 24 h stations.

1469

1470

1471

1472

1473

Appendix

1474

S-Table 1: As Table 3 ~~Table-3~~ and Table 4 ~~Table-4~~ using ERA-Interim MABL height.

1475

	OD [% d ⁻¹]	COL [% d ⁻¹]	CL [% d ⁻¹]	AD [% d ⁻¹]	ODR	CLR	ADR	VMR _{ODR} [ppt]	VMR _{CLR} [ppt]	VMR _A DR [ppt]	MABL-FT Flux [pmol m ⁻² hr ⁻¹]
CHBr₃	87.0	-224.9		144.9	0.43	-0.03	0.60	0.88	-0.07	1.22	4251
	±	±	-7.1	±	±	±	±	±	±	±	±
	124.5	70.7		143.1	0.56	0.01	0.55	1.18	0.04	1.20	1907
CH₂Br₂	39.3	-224.9		186.7	0.20	-0.01	0.80	0.24	-0.01	0.93	2456
	±	±	-1.2	±	±	±	±	±	±	±	±
	40.3	70.7		83.2	0.21	0.00	0.21	0.26	0.00	0.27	921
CH₃I	135.2	-224.9		113.8	0.73	-0.12	0.39	0.28	-0.05	0.14	799
	±	±	-24.0	±	±	±	±	±	±	±	±
	195.0	70.7		220.8	1.06	0.05	1.04	0.39	0.02	0.37	356

1476

Acknowledgements

This work was supported by the EU project SHIVA under grant agreement no. FP7-ENV-2007-1-226224 and by the BMBF grants SHIVA-SONNE 03G0218A and SOPRAN II FKZ 03F0611A. We thank the authorities of Malaysia and the Philippines for the permissions to work in their territorial waters, as well as the SHIVA coordinators Klaus Pfeilsticker and Marcel Dorf and all other SHIVA contributors. We acknowledge the European Centre for medium range weather forecast (ECMWF) for the provision of ERA-Interim reanalysis data and the Lagrangian particle dispersion model FLEXPART used in this publication. We would also like to thank for the support, the captain and crew of R/V SONNE and the pilot in command and crew of R/A FALCON as well as the Projektträger Jülich (PTJ) and the Deutscher Wetterdienst (DWD). E. Atlas was supported by grant #NNX12AH02G from the NASA Upper Atmosphere Research Program. We thank X. Zhu and L. Pope for technical support of canister analysis and C. Marandino for proof reading the manuscript.

REFERENCES

- Aschmann, J., Sinnhuber, B., Chipperfield, M., and Hossaini, R.: Impact of deep convection and dehydration on bromine loading in the upper troposphere and lower stratosphere, *Atmospheric Chemistry and Physics*, 11, 2671-2687, 10.5194/acp-11-2671-2011, 2011.
- Aschmann, J., and Sinnhuber, B.: Contribution of very short-lived substances to stratospheric bromine loading: uncertainties and constraints, *Atmospheric Chemistry and Physics*, 13, 1203-1219, 10.5194/acp-13-1203-2013, 2013.
- Brinckmann, S., Engel, A., Bonisch, H., Quack, B., and Atlas, E.: Short-lived brominated hydrocarbons - observations in the source regions and the tropical tropopause layer, *Atmospheric Chemistry and Physics*, 12, 1213-1228, 10.5194/acp-12-1213-2012, 2012.
- Carpenter, L., and Liss, P.: On temperate sources of bromoform and other reactive organic bromine gases, *Journal of Geophysical Research-Atmospheres*, 105, 20539-20547, 10.1029/2000JD900242, 2000.
- Carpenter, L., Liss, P., and Penkett, S.: Marine organohalogens in the atmosphere over the Atlantic and Southern Oceans, *Journal of Geophysical Research-Atmospheres*, 108, 10.1029/2002JD002769, 2003.
- Carpenter, L. J., Reimann, S., Burkholder, J. B., Clerbaux, C., Hall, B. D., Hossaini, R., Laube, J. C., and Yvon-Lewis, S. A.: Update on Ozone-Depleting Substances (ODSs) and Other Gases of Interest to the Montreal Protocol, in: *Scientific Assessment of Ozone Depletion: 2014*, edited by: Engel, A., and Montzka, S. A., World Meteorological Organization, Geneva, 2014.
- Dee, D., Uppala, S., Simmons, A., Berrisford, P., Poli, P., Kobayashi, S., Andrae, U., Balmaseda, M., Balsamo, G., Bauer, P., Bechtold, P., Beljaars, A., van de Berg, L., Bidlot, J., Bormann, N., Delsol, C., Dragani, R., Fuentes, M., Geer, A., Haimberger, L., Healy, S., Hersbach, H., Holm, E., Isaksen, L., Kallberg, P., Kohler, M., Matricardi, M., McNally, A., Monge-Sanz, B., Morcrette, J., Park, B., Peubey, C., de Rosnay, P., Tavolato, C., Thepaut, J., and Vitart, F.: The ERA-Interim reanalysis: configuration and performance of the data assimilation system, *Quarterly Journal of the Royal Meteorological Society*, 137, 553-597, 10.1002/qj.828, 2011.
- Dix, B., Baidara, S., Bresch, J., Hall, S., Schmidt, K., Wang, S., and Volkamer, R.: Detection of iodine monoxide in the tropical free troposphere, *Proceedings of the National Academy of Sciences of the United States of America*, 110, 2035-2040, 10.1073/pnas.1212386110, 2013.
- Forster, C., Stohl, A., and Seibert, P.: Parameterization of convective transport in a Lagrangian particle dispersion model and its evaluation, *Journal of Applied Meteorology and Climatology*, 46, 403-422, 10.1175/JAM2470.1, 2007.

1521 Fuhlbrügge, S., Krüger, K., Quack, B., Atlas, E., Hepach, H., and Ziska, F.: Impact of the marine atmospheric
 1522 boundary layer conditions on VSLs abundances in the eastern tropical and subtropical North Atlantic Ocean,
 1523 Atmospheric Chemistry and Physics, 13, 6345-6357, 10.5194/acp-13-6345-2013, 2013.
 1524 Fuhlbrügge, S., Quack, B., Atlas, E., Fiehn, A., Hepach, H., and Krüger, K.: Meteorological constraints on oceanic
 1525 halocarbons above the Peruvian Upwelling, Atmos. Chem. Phys. Discuss., 15, 20597–20628, 10.5194/acpd-15-
 1526 20597-2015, 2015.
 1527 Gschwend, P., Macfarlane, J., and Newman, K.: Volatile halogenated organic-compounds released to seawater
 1528 from temperate marine macroalgae, Science, 227, 1033-1035, 10.1126/science.227.4690.1033, 1985.
 1529 Hendon, H., and Woodberry, K.: The diurnal cycle of tropical convection, Journal of Geophysical Research-
 1530 Atmospheres, 98, 16623-16637, 10.1029/93JD00525, 1993.
 1531 Hepach, H., Quack, B., Ziska, F., Fuhlbrügge, S., Atlas, E., Krüger, K., Peeken, I., and Wallace, D. W. R.: Drivers of
 1532 diel and regional variations of halocarbon emissions from the tropical North East Atlantic, Atmos. Chem. Phys.,
 1533 14, 10.5194/acp-14-1255-2014, 2014.
 1534 Hossaini, R., Chipperfield, M., Monge-Sanz, B., Richards, N., Atlas, E., and Blake, D.: Bromoform and
 1535 dibromomethane in the tropics: a 3-D model study of chemistry and transport, Atmospheric Chemistry and
 1536 Physics, 10, 719-735, 10.5194/acp-10-719-2010, 2010.
 1537 Hossaini, R., Mantle, H., Chipperfield, M., Montzka, S., Hamer, P., Ziska, E., Quack, B., Kruger, K., Tegtmeier, S.,
 1538 Atlas, E., Sala, S., Engel, A., Bonisch, H., Keber, T., Oram, D., Mills, G., Ordonez, C., Saiz-Lopez, A., Warwick, N.,
 1539 Liang, Q., Feng, W., Moore, E., Miller, B., Marecal, V., Richards, N., Dorf, M., and Pfeilsticker, K.: Evaluating
 1540 global emission inventories of biogenic bromocarbons, Atmospheric Chemistry and Physics, 13, 11819-11838,
 1541 10.5194/acp-13-11819-2013, 2013.
 1542 Hossaini, R., Chipperfield, M., Montzka, S., Rap, A., Dhomse, S., and Feng, W.: Efficiency of short-lived halogens
 1543 at influencing climate through depletion of stratospheric ozone, Nature Geoscience, 8, 186-190,
 1544 10.1038/NGEO2363, 2015.
 1545 Hughes, C., Johnson, M., von Glasow, R., Chance, R., Atkinson, H., Souster, T., Lee, G., Clarke, A., Meredith, M.,
 1546 Venables, H., Turner, S., Malin, G., and Liss, P.: Climate-induced change in biogenic bromine emissions from
 1547 the Antarctic marine biosphere, Global Biogeochemical Cycles, 26, 10.1029/2012GB004295, 2012.
 1548 Ko, M. K. W., Poulet, G., and Blake, D. R.: Very short-lived halogen and sulfur substances, Scientific assessment
 1549 of ozone depletion: 2002, Global Ozone Research and Monitoring Project. Report No. 47, Chapter 2, World
 1550 Meteorological Organization, Geneva, 2003.
 1551 Krüger, K., and Quack, B.: Introduction to special issue: the TransBrom Sonne expedition in the tropical West
 1552 Pacific, Atmospheric Chemistry and Physics, 13, 9439-9446, 10.5194/acp-13-9439-2013, 2013.
 1553 Lee-Taylor, J., and Redeker, K.: Reevaluation of global emissions from rice paddies of methyl iodide and other
 1554 species, Geophysical Research Letters, 32, 10.1029/2005GL022918, 2005.
 1555 Leedham, E., Hughes, C., Keng, F., Phang, S., Malin, G., and Sturges, W.: Emission of atmospherically significant
 1556 halocarbons by naturally occurring and farmed tropical macroalgae, Biogeosciences, 10, 3615-3633,
 1557 10.5194/bg-10-3615-2013, 2013.
 1558 Lennartz, S. T., Krysztofiak, G., Marandino, C. A., Sinnhuber, B. M., Tegtmeier, S., Ziska, F., Hossaini, R., Krüger,
 1559 K., Montzka, S. A., Atlas, E., Oram, D. E., Keber, T., Bönsch, H., and Quack, B.: Modelling marine emissions and
 1560 atmospheric distributions of halocarbons and dimethyl sulfide: the influence of prescribed water
 1561 concentration vs. prescribed emissions, Atmos. Chem. Phys., 15, 11753-11772, 10.5194/acp-15-11753-2015,
 1562 2015.
 1563 Liss, P. S., and Merlivat, L.: Air-Sea Gas Exchange Rates: Introduction and Synthesis, in: The Role of Air-Sea
 1564 Exchange in Geochemical Cycling, edited by: Buat-Menard, P., Reidel, D., and Norwell, M., Springer
 1565 Netherlands, 113-127, 1986.
 1566 Liu, Y., Yvon-Lewis, S., Thornton, D., Butler, J., Bianchi, T., Campbell, L., Hu, L., and Smith, R.: Spatial and
 1567 temporal distributions of bromoform and dibromomethane in the Atlantic Ocean and their relationship with
 1568 photosynthetic biomass, Journal of Geophysical Research-Oceans, 118, 3950-3965, 10.1002/jgrc.20299, 2013.
 1569 Manley, S., and Dastoor, M.: Methyl-iodide (CH₃I) production by kelp and associated microbes, Marine
 1570 Biology, 98, 477-482, 10.1007/BF00391538, 1988.
 1571 Manley, S. L., and de la Cuesta, J. L.: Methyl iodide production from marine phytoplankton cultures, Limnology
 1572 and Oceanography, 42, 142-147, 1997.
 1573 Margules, M.: Über die Energie der Stürme, K. k. Zentralanstalt für Meteorologie und Erdmagnetismus in Wien,
 1574 1-26, 1905.
 1575 Moncrieff, M., and Miller, M.: Dynamics and simulation of tropical cumulonimbus and squall lines, Quarterly
 1576 Journal of the Royal Meteorological Society, 102, 373-394, 10.1002/qj.49710243208, 1976.

1577 Montzka, S., Butler, J., Hall, B., Mondeel, D., and Elkins, J.: A decline in tropospheric organic bromine,
1578 Geophysical Research Letters, 30, 10.1029/2003GL017745, 2003.

1579 Montzka, S. A., and Reimann, S.: Ozone-depleting substances and related chemicals, Scientific Assessment of
1580 Ozone Depletion: 2010, Global Ozone Research and Monitoring Project – Report No. 52, Geneva, Switzerland,
1581 2011.

1582 Nadzir, M., Phang, S., Abas, M., Rahman, N., Abu Samah, A., Sturges, W., Oram, D., Mills, G., Leedham, E., Pyle,
1583 J., Harris, N., Robinson, A., Ashfold, M., Mead, M., Latif, M., Khan, M., Amiruddin, A., Banan, N., and Hanafiah,
1584 M.: Bromocarbons in the tropical coastal and open ocean atmosphere during the 2009 Prime Expedition
1585 Scientific Cruise (PESC-09), Atmospheric Chemistry and Physics, 14, 8137-8148, 10.5194/acp-14-8137-2014,
1586 2014.

1587 Nightingale, P., Malin, G., Law, C., Watson, A., Liss, P., Liddicoat, M., Boutin, J., and Upstill-Goddard, R.: In situ
1588 evaluation of air-sea gas exchange parameterizations using novel conservative and volatile tracers, Global
1589 Biogeochemical Cycles, 14, 373-387, 10.1029/1999GB900091, 2000.

1590 Quack, B., and Suess, E.: Volatile halogenated hydrocarbons over the western Pacific between 43 degrees and
1591 4 degrees N, Journal of Geophysical Research-Atmospheres, 104, 1663-1678, 10.1029/98JD02730, 1999.

1592 Quack, B., and Wallace, D.: Air-sea flux of bromoform: Controls, rates, and implications, Global Biogeochemical
1593 Cycles, 17, 10.1029/2002GB001890, 2003.

1594 Quack, B., Atlas, E., Petrick, G., and Wallace, D.: Bromoform and dibromomethane above the Mauritanian
1595 upwelling: Atmospheric distributions and oceanic emissions, Journal of Geophysical Research-Atmospheres,
1596 112, 10.1029/2006JD007614, 2007.

1597 Quack, B., Krüger, K., Atlas, E., Tegtmeier, S., Großmann, K., Rex, M., von Glasow, R., Sommariva, R., and
1598 Wallace, D.: Halocarbon sources and emissions over the Western Pacific, oral presentation on 05.04.2011,
1599 EGU, Vienna, Austria, 2011.

1600 Redeker, K., Meinardi, S., Blake, D., and Sass, R.: Gaseous emissions from flooded rice paddy agriculture,
1601 Journal of Geophysical Research-Atmospheres, 108, 10.1029/2002JD002814, 2003.

1602 Ren, Y., Baumann, R., and Schlager, H.: An airborne perfluorocarbon tracer system and its first application for a
1603 Lagrangian experiment, 7, 6791-6822, 10.5194/amtd-7-6791-2014, 2014.

1604 Rex, M., Wohltmann, I., Ridder, T., Lehmann, R., Rosenlof, K., Wennberg, P., Weisenstein, D., Notholt, J.,
1605 Kruger, K., Mohr, V., and Tegtmeier, S.: A tropical West Pacific OH minimum and implications for stratospheric
1606 composition, Atmospheric Chemistry and Physics, 14, 4827-4841, 10.5194/acp-14-4827-2014, 2014.

1607 Richter, U., and Wallace, D.: Production of methyl iodide in the tropical Atlantic Ocean, Geophysical Research
1608 Letters, 31, 10.1029/2004GL020779, 2004.

1609 Saiz-Lopez, A., and von Glasow, R.: Reactive halogen chemistry in the troposphere, Chemical Society Reviews,
1610 41, 6448-6472, 10.1039/c2cs35208g, 2012.

1611 Saiz-Lopez, A., Fernandez, R., Ordóñez, C., Kinnison, D., Martin, J., Lamarque, J., and Tilmes, S.: Iodine
1612 chemistry in the troposphere and its effect on ozone, Atmospheric Chemistry and Physics, 14, 13119-13143,
1613 10.5194/acp-14-13119-2014, 2014.

1614 Sala, S., Bonisch, H., Keber, T., Oram, D., Mills, G., and Engel, A.: Deriving an atmospheric budget of total
1615 organic bromine using airborne in situ measurements from the western Pacific area during SHIVA,
1616 Atmospheric Chemistry and Physics, 14, 6903-6923, 10.5194/acp-14-6903-2014, 2014.

1617 Schauffler, S., Atlas, E., Blake, D., Flocke, F., Lueb, R., Lee-Taylor, J., Stroud, V., and Travnicek, W.: Distributions
1618 of brominated organic compounds in the troposphere and lower stratosphere, Journal of Geophysical
1619 Research-Atmospheres, 104, 21513-21535, 10.1029/1999JD900197, 1999.

1620 Seibert, P., Beyrich, F., Gryning, S., Joffre, S., Rasmussen, A., and Tercier, P.: Review and intercomparison of
1621 operational methods for the determination of the mixing height, Atmospheric Environment, 34, 1001-1027,
1622 10.1016/S1352-2310(99)00349-0, 2000.

1623 Solomon, S., Garcia, R., and Ravishankara, A.: On the role of iodine in ozone depletion, Journal of Geophysical
1624 Research-Atmospheres, 99, 20491-20499, 10.1029/94JD02028, 1994.

1625 Solomon, S.: Stratospheric ozone depletion: A review of concepts and history, Reviews of Geophysics, 37, 275-
1626 316, 10.1029/1999RG900008, 1999.

1627 Sorensen, J.: Sensitivity of the DERMA long-range gaussian dispersion model to meteorological input and
1628 diffusion parameters, Atmospheric Environment, 32, 4195-4206, 10.1016/S1352-2310(98)00178-2, 1998.

1629 Stohl, A., Hittenberger, M., and Wotawa, G.: Validation of the Lagrangian particle dispersion model FLEXPART
1630 against large-scale tracer experiment data, Atmospheric Environment, 32, 4245-4264, 10.1016/S1352-
1631 2310(98)00184-8, 1998.

1632 Stohl, A., and Thomson, D.: A density correction for Lagrangian particle dispersion models, Boundary-Layer
1633 Meteorology, 90, 155-167, 10.1023/A:1001741110696, 1999.

Stohl, A., and Trickl, T.: A textbook example of long-range transport: Simultaneous observation of ozone maxima of stratospheric and North American origin in the free troposphere over Europe, *Journal of Geophysical Research-Atmospheres*, 104, 30445-30462, 10.1029/1999JD900803, 1999.

Stohl, A., Forster, C., Frank, A., Seibert, P., and Wotawa, G.: Technical note: The Lagrangian particle dispersion model FLEXPART version 6.2, *Atmospheric Chemistry and Physics*, 5, 2461-2474, 2005.

Stull, R.: *An Introduction to Boundary Layer Meteorology*, Kluwer Academic Publishers, Dordrecht, 1988.

Tegtmeier, S., Krüger, K., Quack, B., Atlas, E. L., Pisso, I., Stohl, A., and Yang, X.: Emission and transport of bromocarbons: from the West Pacific ocean into the stratosphere, *Atmos. Chem. Phys.*, 12, 10633-10648, 10.5194/acp-12-10633-2012, 2012.

Tegtmeier, S., Krüger, K., Quack, B., Atlas, E., Blake, D., Boenisch, H., Engel, A., Hepach, H., Hossaini, R., Navarro, M., Raimund, S., Sala, S., Shi, Q., and Ziska, E.: The contribution of oceanic methyl iodide to stratospheric iodine, *Atmospheric Chemistry and Physics*, 13, 11869-11886, 10.5194/acp-13-11869-2013, 2013.

Thompson, R., and Edwards, R.: An overview of environmental conditions and forecast implications of the 3 May 1999 tornado outbreak, *Weather and Forecasting*, 15, 682-699, 10.1175/1520-0434(2000)015<0682:AOOECA>2.0.CO;2, 2000.

Tie, X., Madronich, S., Walters, S., Zhang, R., Rasch, P., and Collins, W.: Effect of clouds on photolysis and oxidants in the troposphere, *Journal of Geophysical Research-Atmospheres*, 108, 10.1029/2003JD003659, 2003.

Troen, I., and Mahrt, L.: A simple-model of the atmospheric boundary-layer: Sensitivity to surface evaporation, *Boundary-Layer Meteorology*, 37, 129-148, 10.1007/BF00122760, 1986.

Vogelezang, D., and Holtslag, A.: Evaluation and model impacts of alternative boundary-layer height formulations, *Boundary-Layer Meteorology*, 81, 245-269, 10.1007/BF02430331, 1996.

von Glasow, R., von Kuhlmann, R., Lawrence, M., Platt, U., and Crutzen, P.: Impact of reactive bromine chemistry in the troposphere, *Atmospheric Chemistry and Physics*, 4, 2481-2497, 2004.

Wanninkhof, R., and McGillis, W.: A cubic relationship between air-sea CO₂ exchange and wind speed, *Geophysical Research Letters*, 26, 1889-1892, 10.1029/1999GL900363, 1999.

Worton, D., Mills, G., Oram, D., and Sturges, W.: Gas chromatography negative ion chemical ionization mass spectrometry: Application to the detection of alkyl nitrates and halocarbons in the atmosphere, *Journal of Chromatography a*, 1201, 112-119, 10.1016/j.chroma.2008.06.019, 2008.

Yang, X., Cox, R., Warwick, N., Pyle, J., Carver, G., O'Connor, F., and Savage, N.: Tropospheric bromine chemistry and its impacts on ozone: A model study, *Journal of Geophysical Research-Atmospheres*, 110, 10.1029/2005JD006244, 2005.

Yang, X., Abraham, N., Archibald, A., Braesicke, P., Keeble, J., Telford, P., Warwick, N., and Pyle, J.: How sensitive is the recovery of stratospheric ozone to changes in concentrations of very short-lived bromocarbons?, *Atmospheric Chemistry and Physics*, 14, 10431-10438, 10.5194/acp-14-10431-2014, 2014.

Yokouchi, Y., Mukai, H., Yamamoto, H., Otsuki, A., Saitoh, C., and Nojiri, Y.: Distribution of methyl iodide, ethyl iodide, bromoform, and dibromomethane over the ocean (east and southeast Asian seas and the western Pacific), *Journal of Geophysical Research-Atmospheres*, 102, 8805-8809, 10.1029/96JD03384, 1997.

Yokouchi, Y., Hasebe, F., Fujiwara, M., Takashima, H., Shiotani, M., Nishi, N., Kanaya, Y., Hashimoto, S., Fraser, P., Toom-Sauntry, D., Mukai, H., and Nojiri, Y.: Correlations and emission ratios among bromoform, dibromochloromethane, and dibromomethane in the atmosphere, *Journal of Geophysical Research-Atmospheres*, 110, 10.1029/2005JD006303, 2005.

Ziska, F., Quack, B., Abrahamsson, K., Archer, S., Atlas, E., Bell, T., Butler, J., Carpenter, L., Jones, C., Harris, N., Hepach, H., Heumann, K., Hughes, C., Kuss, J., Krüger, K., Liss, P., Moore, R., Orlikowska, A., Raimund, S., Reeves, C., Reifenhäuser, W., Robinson, A., Schall, C., Tanhua, T., Tegtmeier, S., Turner, S., Wang, L., Wallace, D., Williams, J., Yamamoto, H., Yvon-Lewis, S., and Yokouchi, Y.: Global sea-to-air flux climatology for bromoform, dibromomethane and methyl iodide, *Atmospheric Chemistry and Physics*, 13, 8915-8934, 10.5194/acp-13-8915-2013, 2013.

Figures

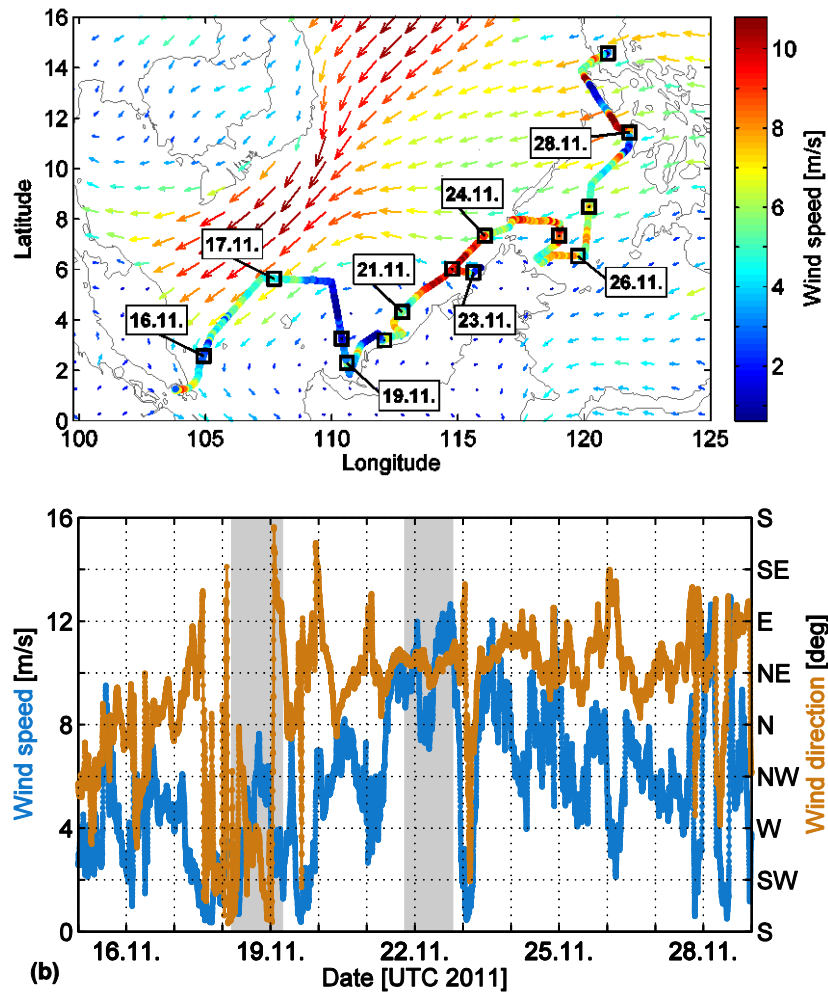


Figure 1-a-b: (a) ERA-Interim mean wind field November 15 – 30, 2011 (arrows) and 10 minute running mean of wind speed observed on R/V SONNE as the cruise track. The black squares show the ships position at 00 UTC each day. (b) Time series of wind speed (blue) and wind direction (orange) measured on R/V SONNE. The data are averaged by a 10 minute running mean. The two shaded areas (light grey) in the background show the 24 h stations.

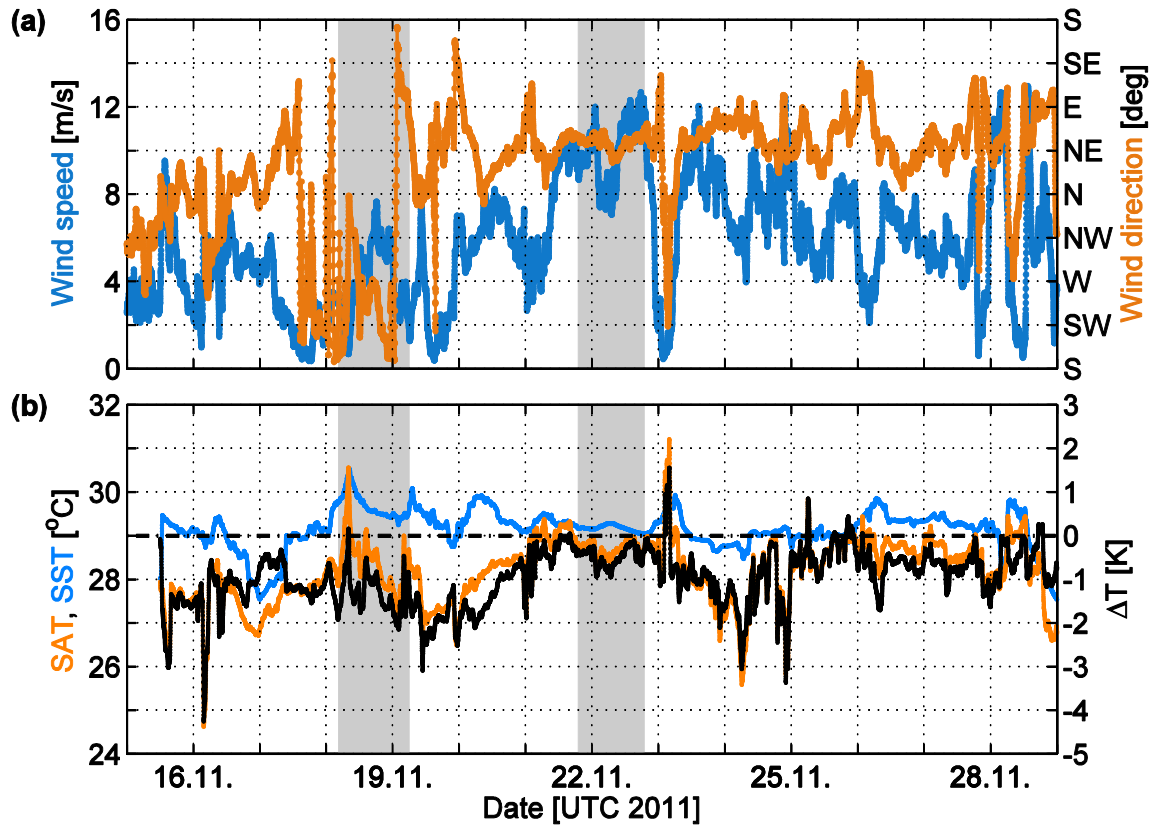


Figure 2 a-b: (a) wind speed (blue) and wind direction (orange) measured on R/V SONNE. The data are averaged by a 10-minute running mean. The two shaded areas (light grey) in the background show the 24 h stations. (b) air surface air temperature (SAT, 10-minute running mean, orange) and sea surface temperature (10-minute running mean SST, blue) as observed on R/V SONNE. The temperature difference of air and water temperature SAT and SST (ΔT) is given on the right scale in (b). For the temperature difference, a ΔT of 0 K is given by dashed line. The shaded areas (grey) in the background show the 24 h stations. The data are averaged by a 10-minute running mean.

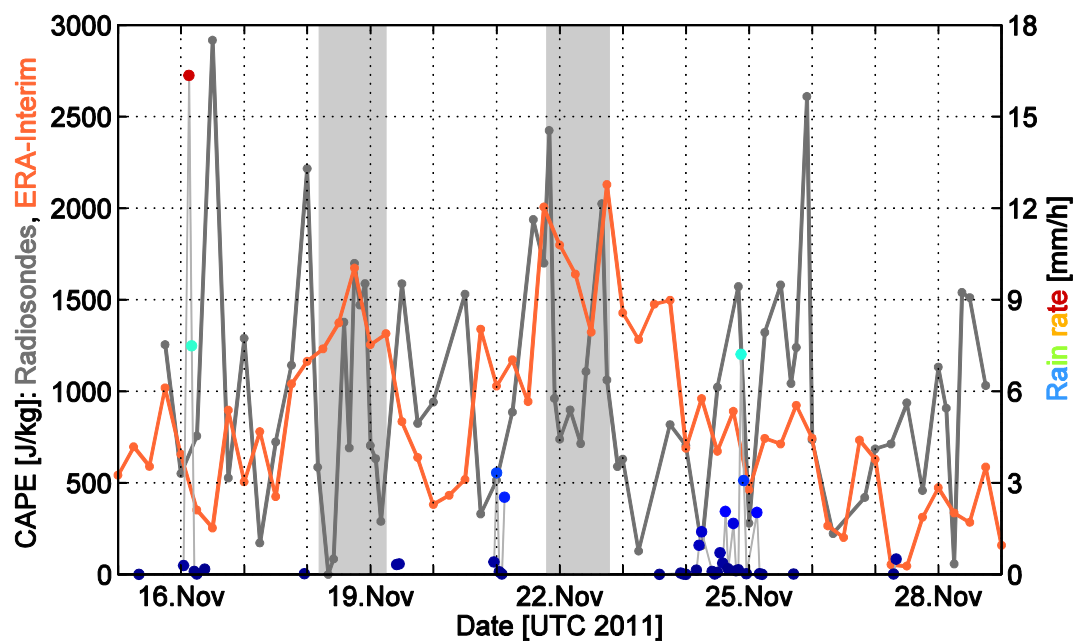


Figure 3: Left scale: convective available potential energy (CAPE) from radiosondes on R/V SONNE (grey) and ERA-Interim (orange). Right scale: Rain rate (colored dots) during the cruise, observed by an optical disdrometer (ODM 470) on R/V SONNE. The two shaded areas (light grey) in the background show the 24 h stations.

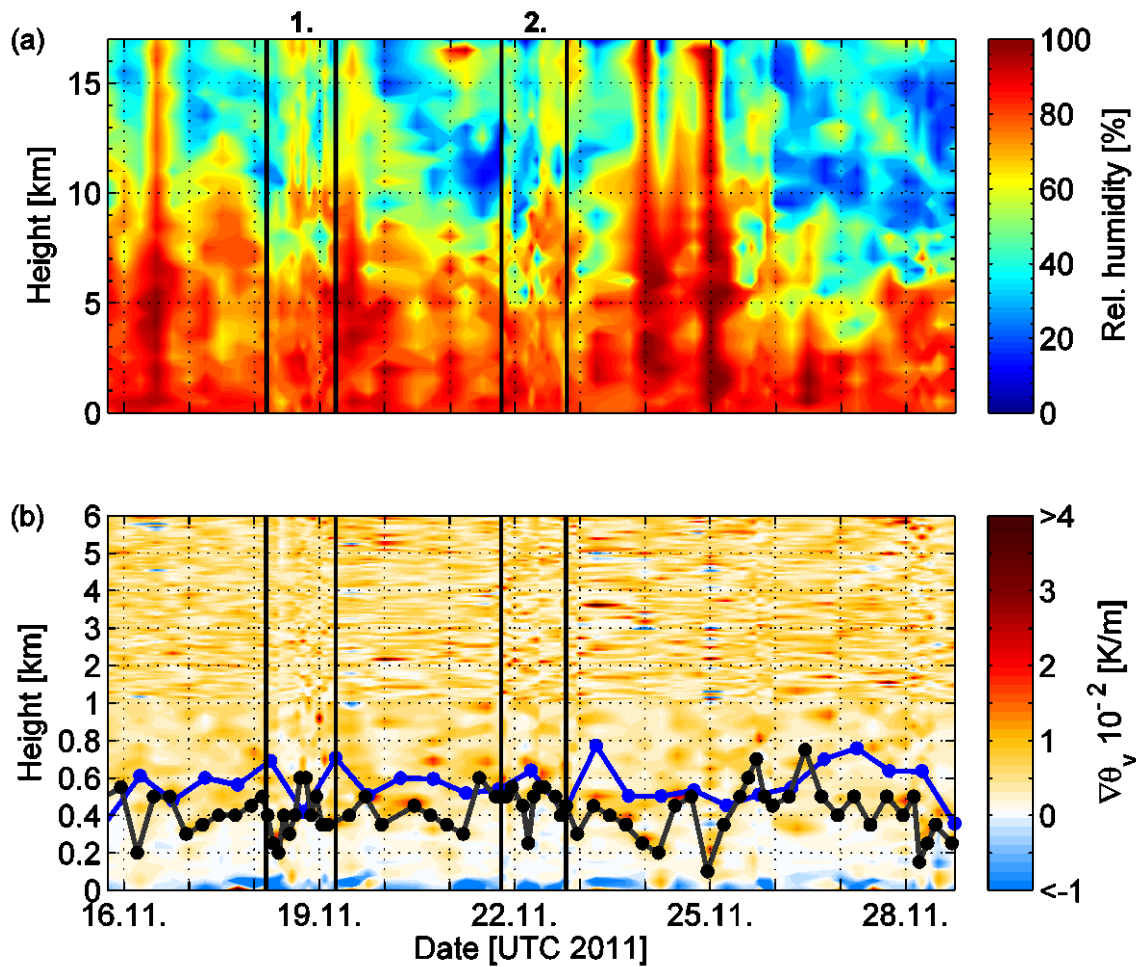


Figure 3: (a) Relative humidity by radiosondes up to 17 km height, the mean cold point tropopause level. The dashed lines and the two numbers above the figure indicate the two 24 h stations. (b) Virtual potential temperature gradient as indicator for atmospheric stability (red for stable, white for neutral and blue for unstable) with MABL height from radiosondes (black curve) and from ERA-Interim (blue curve). The y axis is non-linear. The lower 1 km is enlarged to display the stability around the MABL height. The vertical lines and the two numbers above the figures indicate the two 24 h stations.

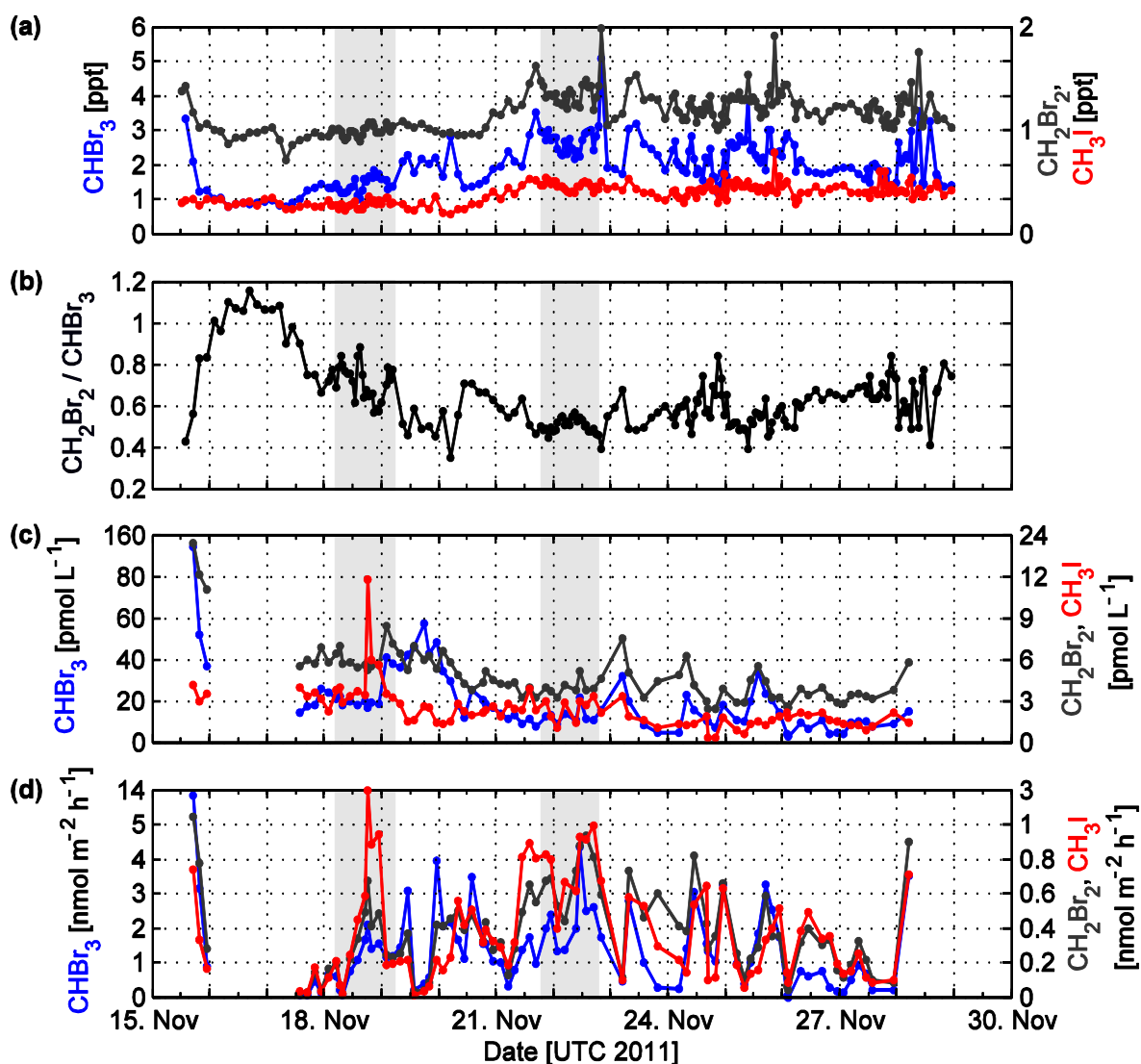


Figure 4 a-d: (a) Atmospheric mixing ratios of CHBr_3 (blue), CH_2Br_2 (dark grey) and CH_3I (red) measured on R/V SONNE. (b) Concentration ratio of CH_2Br_2 and CHBr_3 on R/V SONNE. (c) Water concentrations of CH_3I , CHBr_3 and CH_2Br_2 measured on R/V SONNE. (d) Emissions—Calculated emissions of CH_3I , CHBr_3 , CH_2Br_2 and CH_3I from atmospheric and water samples measured on R/V SONNE. The two shaded areas (light grey) in the background show the 24 h stations. Y-axis for (c) and (d) are non-linear.

Table 1: Mean \pm standard deviation and range of atmospheric mixing ratios observed on R/V SONNE (195 data points) and R/A FALCON (GhOST-MS with 513 and WASP GC/MS with 202 data points) in the MABL and the FT, water concentrations observed by on R/V SONNE and the computed sea – air fluxes. MABL and FT mixing ratios for bromoform and dibromomethane on R/A FALCON are adopted from Sala et al. (2014) and Tegtmeier et al. (2013). The R/A FALCON MABL height was set analysed to be 450 m (Sala et al., 2014). The last line gives the sea – air flux computed from R/V SONNE mixing ratios for all three compounds.

				CHBr ₃ Bromoform m	CH ₂ Br ₂ Dibromo methane	CH ₃ I Methyl iodide
Atmosph. mixing ratios [ppt]	R/V SONNE			2.08 ± 1.36 [0.79 – 5.07]	1.17 ± 0.19 [0.71 - 1.98]	0.39 ± 0.09 [0.19 – 0.78]
	R/A FALCON	GhOST	MABL	1.43 ± 0.53 [0.42 – 3.42]	1.19 ± 0.21 [0.58 – 1.89]	0. 59 ± 0.30 [0.29 - 3.23]
			FT	0.56 ± 0.17 [0.16 – 2.15]	0.87 ± 0.12 [0.56 – 1.54]	0.26 ± 0.11 [0.08 – 0.80]
		WASP	MABL	1.90 ± 0.55 [0.99 – 3.78]	1.15 ± 0.14 [0.85 – 1.59]	/
			FT	1.17 ± 0.50 [0.43 – 3.22]	0.88 ± 0.14 [0.46 – 1.36]	/
	Water concentrations [pmol L ⁻¹]				19.94 ± 17.90 [2.80 – 136.91]	4.99 ± 2.59 [2.43 – 21.82]
Sea – air flux [pmol m ⁻² h ⁻¹]				1486 ± 1718 [-8 – 13149]	405 ± 349 [16 - 2210]	433 ± 482 [13 - 2980]

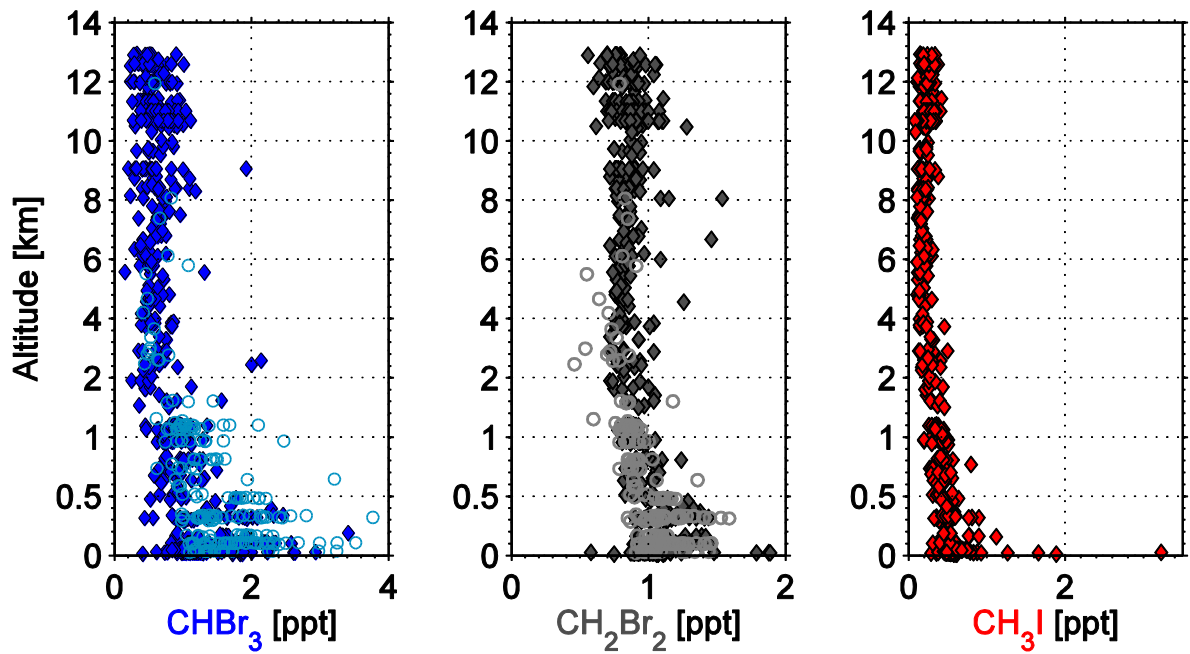


Figure 5: Vertical distribution CHBr_3 bromoform (CHBr_3 , blue), CH_2Br_2 dibromomethane (CH_2Br_2 , grey) and CH_3I methyl iodide (CH_3I , red) mixing ratios measured in-situ by GhOST (diamonds) and with flasks by WASP (circles) on R/A FALCON. CH_3I Methyl iodide was only measured in-situ by GhOST. The lower 2 km are non-linear displayed.

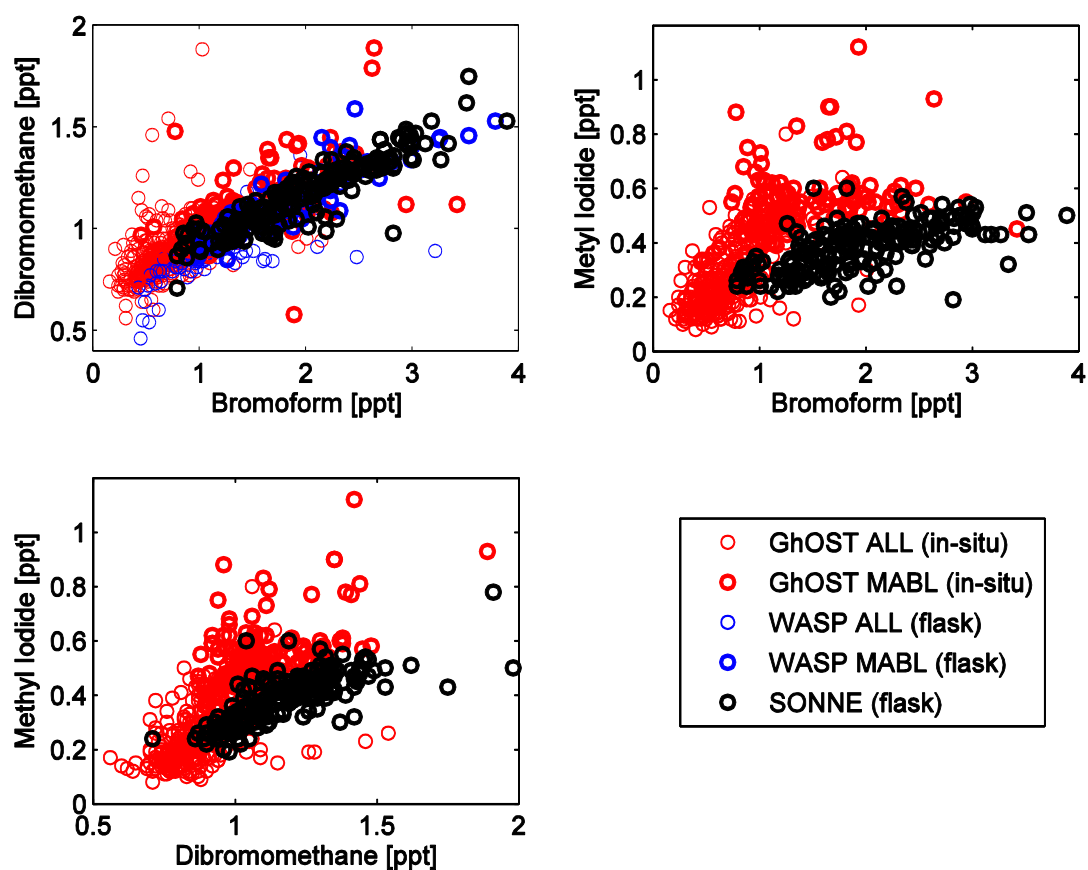


Figure 6: Correlation of bromoform and CH_2Br_2 dibromomethane (upper left), bromoform and CH_3I methyl iodide (upper right), and CH_2Br_2 dibromomethane and CH_3I methyl iodide (lower left) from GhOST and WASP for all heights (ALL) and only within the MABL (MABL) and from R/V SONNE.

Table 2: Mean atmospheric mixing ratios of CHBr_3 bromoform, CH_2Br_2 dibromomethane and CH_3I methyl iodide observed on R/V SONNE and R/A FALCON during two case studies on 19.11.2011 at 3.2° N and 112.5° E and on 21.11.2011 at 4.6° N and 113.0° E. During the two meetings two (one) measurements have been taken by R/V SONNE, 20 (5) measurements on R/A FALCON by GhOST and 17 (21) by WASP.

		CHBr_3 Bromoform [ppt]	CH_2Br_2 Dibromomethane [ppt]	CH_3I Methyl iodide [ppt]
November 19, 2011	R/V SONNE	1.37	0.99	0.29
	R/A FALCON: GhOST / WASP	1.02 / 1.37	0.94 / 1.03	0.45 / -
November 21, 2011	R/V SONNE	2.05	1.08	0.28
	R/A FALCON: GhOST / WASP	1.63 / 2.00	1.31 / 1.08	0.82 / -

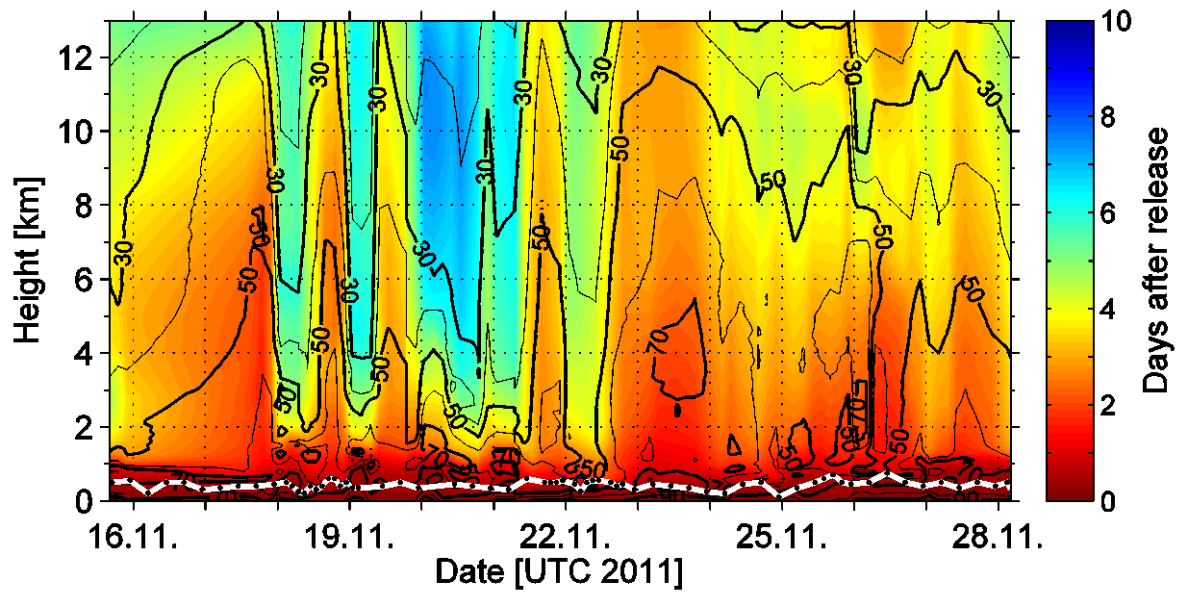


Figure 7: Forward trajectory runs along the cruise track with FLEXPART using ERA-Interim data. The black contour lines show the mean amount of trajectories (in %) reaching this height within the specific time (colour shading). The white line indicates the radiosonde MABL height.

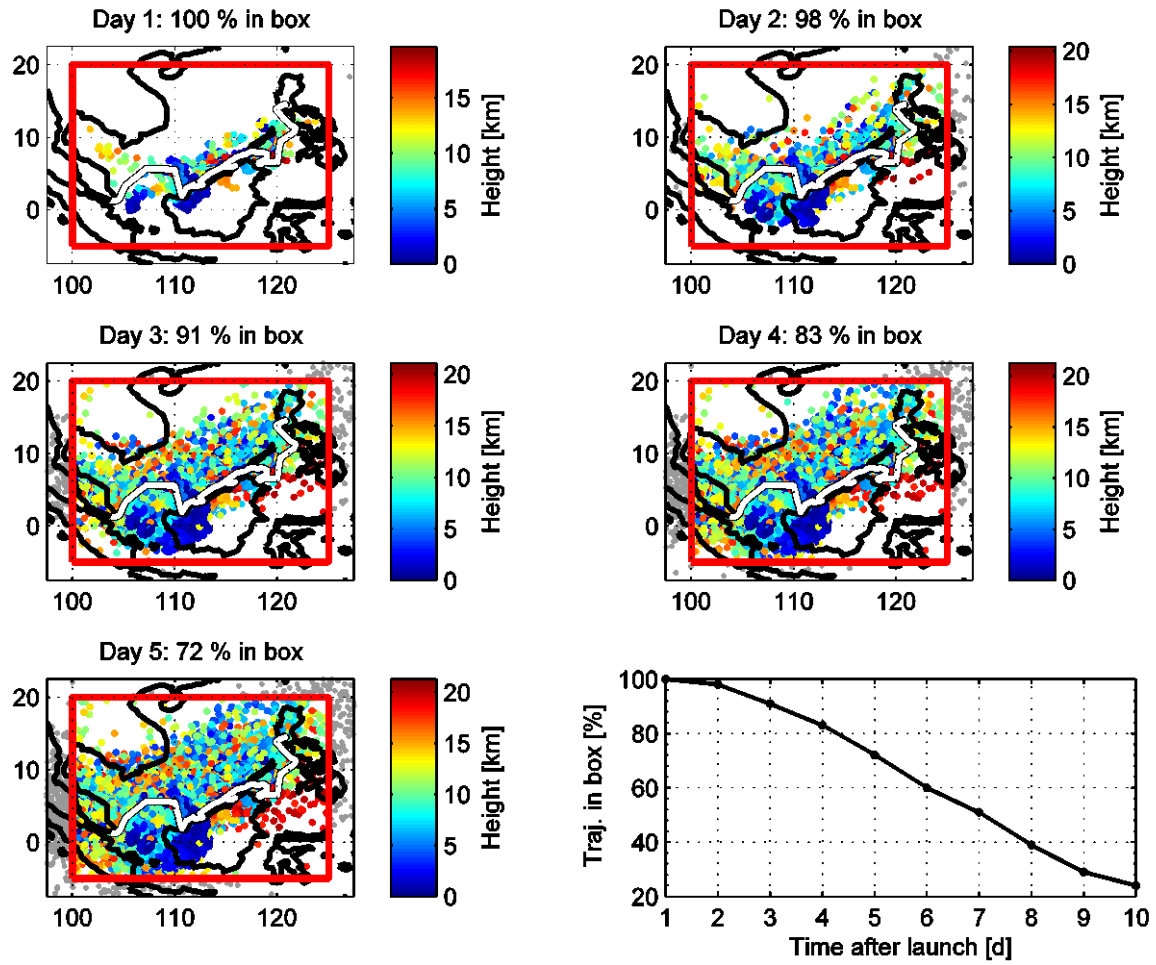


Figure 8: Horizontal distribution, altitude and amount of trajectories ~~with~~ over time during the cruise. The red box represents the South China and Sulu Seas area. The lower right plot shows the amount of trajectories that remain in the box with time from all trajectory releases.

1766 Table 3: Mean \pm standard deviation of Oceanic Delivery (OD), CONvective Loss (COL),
 1767 Chemical Loss (CL), Advective Delivery (AD), Oceanic Delivery Ratio (ODR), Chemical
 1768 Loss Ratio (CLR), and Advective Delivery Ratio (ADR) for ~~bromoform~~ (CHBr_3),
 1769 ~~dibromomethane~~ (CH_2Br_2) and ~~methyl iodide~~ (CH_3I).

	OD [% d ⁻¹]	COL [% d ⁻¹]	CL [% d ⁻¹]	AD [% d ⁻¹]	ODR	CLR	ADR
CHBr₃	116.4 \pm 163.6	-307.6 \pm 124.3	 -7.1	198.2 \pm 199.7	0.45 \pm 0.55	-0.03 \pm 0.01	0.58 \pm 0.55
CH₂Br₂	54.2 \pm 66.7	-307.6 \pm 124.3	 -1.2	254.6 \pm 131.9	0.20 \pm 0.21	-0.00 \pm 0.00	0.80 \pm 0.21
CH₃I	166.5 \pm 185.8	-307.6 \pm 124.3	 -24.0	165.2 \pm 242.3	0.74 \pm 1.05	-0.09 \pm 0.04	0.35 \pm 1.02

1770

1771

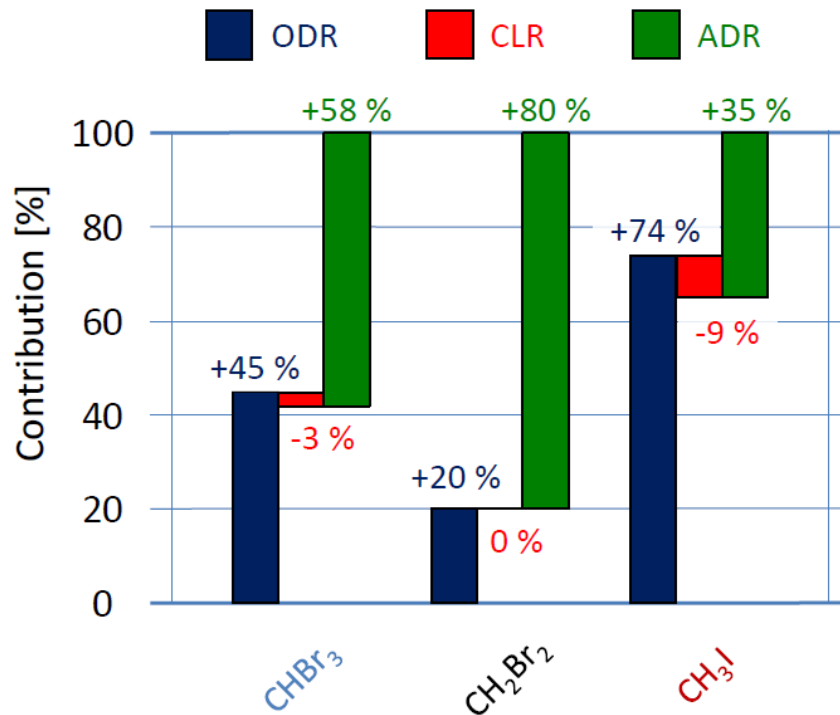


Figure 9: Budgets of the Oceanic Delivery Ratio (ODR, blue), Chemical Loss Ratio (CLR, red) and Advective Delivery Ratio (ADR, green) of CHBr₃, CH₂Br₂ and CH₃I. Time-series of oceanic delivery (OD) to MABL concentration in % per day (blue), Convective Loss (COL) from the MABL to the FT in % per day (orange) and the Oceanic Delivery Ratio (ODR, black) for bromoform (upper plot), dibromomethane (centre plot) and methyl iodide (lower plot).

Table 4: Mean \pm standard deviation of observed Volume Mixing Ratios in the MABL on R/V SONNE (VMR_{MABL}) versus the amount of VMR originating from oceanic emissions (VMR_{ODR}), chemically degraded according to the specific lifetime (VMR_{CLR}), originating from advection (VMR_{ADR}) and the Flux from the MABL into the FT ($\text{Flux}_{\text{MABL-FT}}$) for ~~bromoform~~ (CHBr_3), ~~dibromomethane~~ (CH_2Br_2) and ~~methyl iodide~~ (CH_3I).

	VMR_{MABL} [ppt]	VMR_{ODR} [ppt]	VMR_{CLR} [ppt]	VMR_{ADR} [ppt]	$\text{Flux}_{\text{MABL-FT}}$ [$\text{pmol m}^{-2} \text{hr}^{-1}$]
CHBr₃	2.08	0.89	-0.06	1.18	4240
	\pm	\pm	\pm	\pm	\pm
	1.36	1.12	0.04	1.20	1889
CH₂Br₂	1.17	0.25	-0.01	0.92	2419
	\pm	\pm	\pm	\pm	\pm
	0.19	0.26	0.00	0.27	929
CH₃I	0.39	0.28	-0.04	0.13	865
	\pm	\pm	\pm	\pm	\pm
	0.09	0.40	0.02	0.37	373

1787 Table 5: Correlation coefficients between wind speed and VSLS MABL mixing ratios
 1788 (VMR_{MABL}), the Oceanic Delivery (OD), the COnductive Loss to the FT (COL), the
 1789 Advective Delivery (AD), computed as the residual of OD, and the mixing ratios originating
 1790 from the OD (VMR_{ODR}) and from the AD (VMR_{ADR}). Bold numbers are significant at the 95
 1791 % (p-value).

<i>Wind speed</i>	CHBr₃Bromoform	CH₂Br₂Dibromomethane	CH₃I Methyl iodide
VMR_{MABL}	0.55	0.57	0.56
OD	0.31	0.48	0.52
COL	-0.33		
AD	-0.46	0.56	-0.57
VMR_{ODR}	0.52	0.72	0.62
VMR_{ADR}	-0.17	-0.31	-0.49

1792

1793

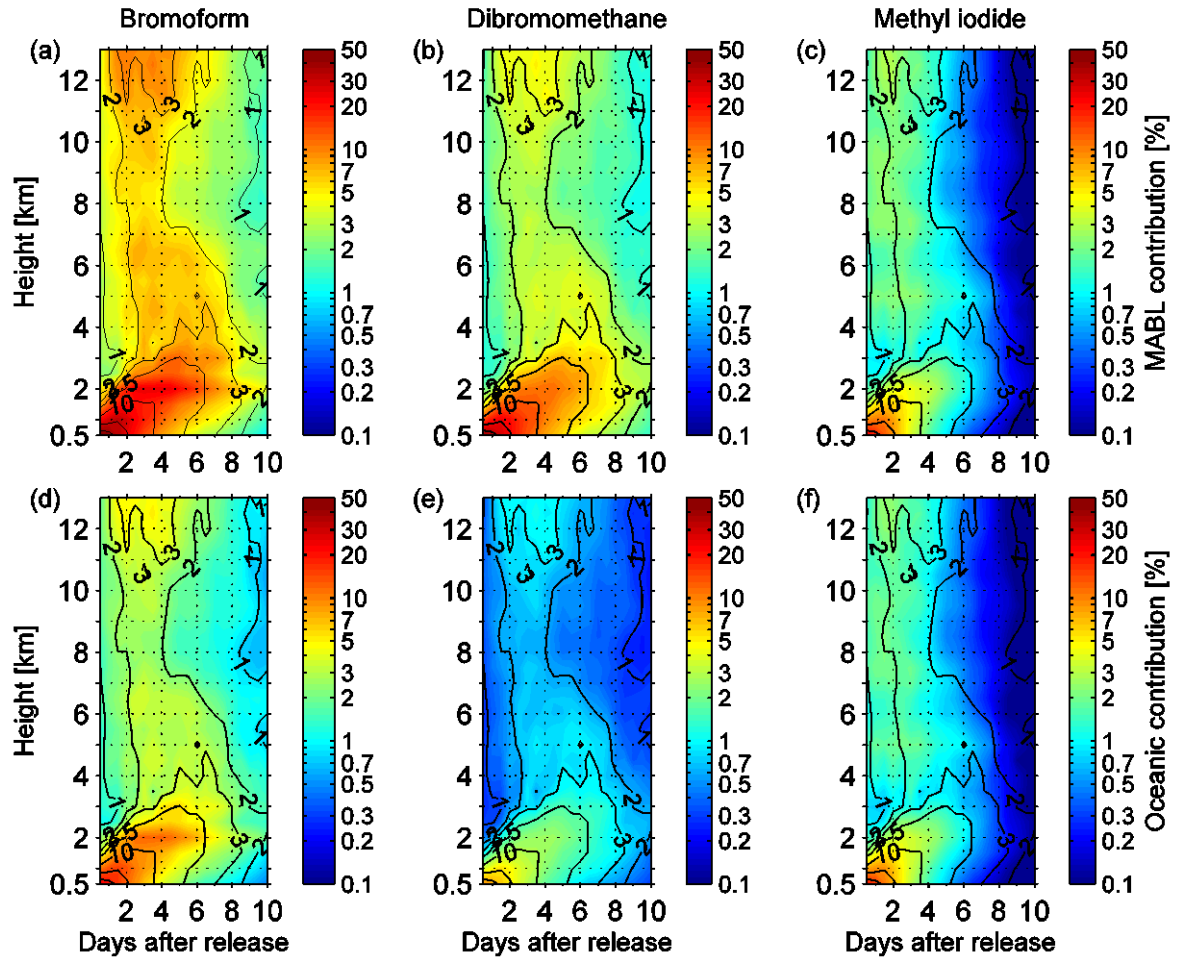


Figure 10: Mean MABL air contribution (upper-plots a – c) and oceanic contribution (lower-plots d – f) to observed FT mixing ratios observed by R/A FALCON for three VSLs. The black contour lines show the mean portion of MABL air masses in the FT [%], the colours show the oceanic contribution to the observed compounds in the FT at specific height and day after release [%] including chemical degradation, the loss out of the South China Sea area with time and the vertical density driven extension of MABL air masses. The scale of the coloured contour is logarithmic.

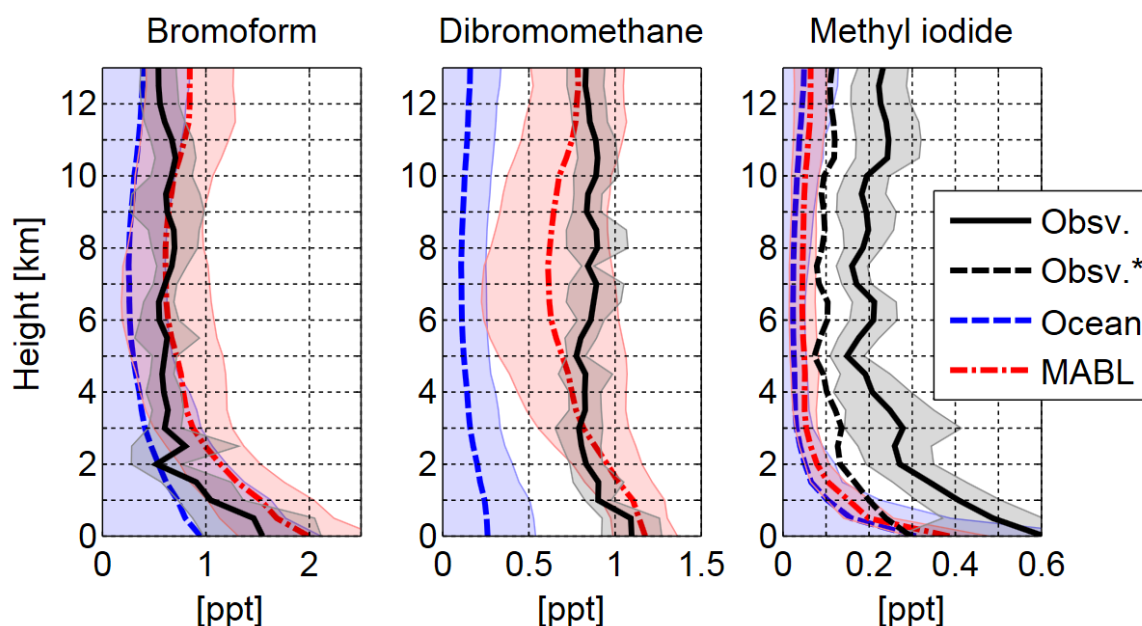


Figure 11: Mean FT mixing ratios (solid lines) and 1 standard deviation (shaded areas) from in-situ and flask observations observed-on by R/A FALCON (Obsv., black) versus simulated mean FT mixing ratios from MABL air (MABL, red) and oceanic emissions (Ocean, blue) observed by R/V SONNE. R/A FALCON in-situ observations have been adjusted for CH_3I methyl iodide (Obsv.*, dashed black) according to measurements deviations during the meetings of R/V SONNE and R/A FALCON (compare Table 2 Table 2; Section 4.34.3).